UNCLASSIFIED

SECURITY CLASSIFICATION OF THIS PAGE *(When Data Entered)*

REPORT DOCUMENTATION PAGE

READ INSTRUCTIONS BEFORE COMPLETING FORM

1. REPORT NUMBER: TR-3903	2. GOVT ACCESSION NO.
3. RECIPIENT'S CATALOG NUMBER	
4. TITLE *(and Subtitle)*: SIGNIFICANT EARLY-TIME TRANSIENT PROJECTILE ACCELERATION WITH CONCOMITANT MINIMAL PRESSURE WAVES.	5. TYPE OF REPORT & PERIOD COVERED: Final, Oct 77-May 78
	6. PERFORMING ORG. REPORT NUMBER
7. AUTHOR(s): C. T. Boyer, Jr.	8. CONTRACT OR GRANT NUMBER(s)
9. PERFORMING ORGANIZATION NAME AND ADDRESS: Naval Surface Weapons Center (G33), Dahlgren, VA 22448	10. PROGRAM ELEMENT, PROJECT, TASK AREA & WORK UNIT NUMBERS: 64602N, S03O5AA, S03O5AA001, CG21BCG01
11. CONTROLLING OFFICE NAME AND ADDRESS: Naval Sea Systems Command, Washington, DC 20360	12. REPORT DATE: November 1978
	13. NUMBER OF PAGES: 47
14. MONITORING AGENCY NAME & ADDRESS *(if different from Controlling Office)*: NSWC/DL-TR-3903	15. SECURITY CLASS. *(of this report)*: UNCLASSIFIED
	15a. DECLASSIFICATION/DOWNGRADING SCHEDULE

16. DISTRIBUTION STATEMENT *(of this Report)*

Approved for public release; distribution unlimited.

17. DISTRIBUTION STATEMENT *(of the abstract entered in Block 20, if different from Report)*

18. SUPPLEMENTARY NOTES

19. KEY WORDS *(Continue on reverse side if necessary and identify by block number)*

projectile response
pressure waves
initial reverse pressure difference
rapid ignition propagation igniter
fast Fourier transform analysis
instrumented projectile
open-air tests
inert-bed tests

20. ABSTRACT *(Continue on reverse side if necessary and identify by block number)*

Recent tests have demonstrated that severe early-time transient projectile accelerations can be produced by a propelling charge assembly that generates only minimal traveling pressure waves in the chamber. Five igniter designs consisting of four rapid ignition propagation (RIP) igniters and one standard black powder igniter were tested in the new Navy 8-in. Major-Caliber Lightweight Gun using simulated 8-in. Extended-Range Guided Projectiles. The

DD FORM 1 JAN 73 1473 EDITION OF 1 NOV 65 IS OBSOLETE
S/N 0102-LF-014-6601

UNCLASSIFIED
SECURITY CLASSIFICATION OF THIS PAGE *(When Data Entered)*

391 578

20. (Continued)

magnitude of the early-time projectile setback acceleration, when firing the HIVELITE-ignited charges, was an order of magnitude less than that experienced with charges ignited by the other igniters. Gun chamber pressures measured during these tests showed that pressure waves were minimal for all of the igniters. Analysis of these pressure records produced no evidence that the observed high level projectile loading should be expected. Hence, the projectile loading attributed to propellant grain and case plug impact was substantial even when overall pressure gradients were minimal. Since projectile loading cannot always be deduced from chamber pressure data alone, projectile loading must be measured in live propellant bed tests in order to determine whether serious setback loading is imparted to the projectile.

FOREWORD

This technical report summarizes the work conducted in the development of an igniter for incorporation in the EX 91 Mod 0 charge assembly. This charge assembly was intended for use with the 8-in. Extended-Range Guided Projectile in the Mk 71 Major-Caliber Lightweight Gun. Actual gunfire tests were conducted where the pressure distribution in the chamber and the projectile setback acceleration were measured for the first 8 ms in the interior ballistic event. The resulting pressure waves and projectile loading were evaluated for each type of igniter tested. These test results demonstrated that the magnitude of the pressure waves does not always correlate with the magnitude of the early-time transient projectile loading. Hence, the absence of pressure waves does not ensure against severe projectile loading.

This report has been reviewed and approved by D. R. McClure, Dr. J. L. East, and T. N. Tschirn, Propulsion Branch; K. G. Thorsted, Head, Propulsion Branch; and C. A. Cooper, Head, Gun Systems and Munitions Division.

Released by:

R. L. Hicks

CDR R. L. HICKS
Assistant for Weapons Systems
Weapons Systems Department

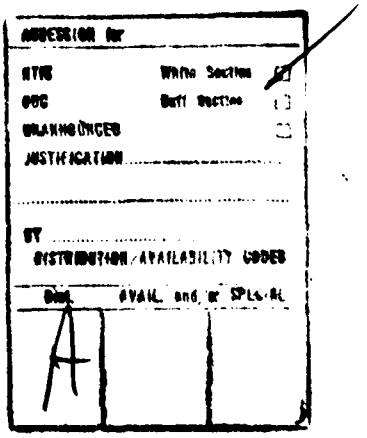

CONTENTS

ILLUSTRATIONS

INTRODUCTION

The guidance and fuzing components in an 8-in. Extended-Range Guided Projectile (ERGP) require a low-loading-condition gun launch with a maximum rigid-body setback acceleration of 4200 g, a much lower requirement than for the standard ballistic ammunition. This low value of maximum rigid-body acceleration indicates that careful attention should be given to the early-time transient loads produced by the charge assembly. During launch, forces are applied to the projectile by the gun chamber gas pressure and the impact of the propellant grains and case closure plug on the base of the projectile. Existing techniques are not sufficient to permit the determination of total projectile loading from the analysis of chamber pressure data alone. Hence, the actual measurement of the projectile response is the only available method to ascertain the level of acceleration experienced by the projectile.

The magnitude of pressure waves in the chamber has been correlated with other ballistic anomalies such as projectile muzzle velocity variation and breech blow malfunctions. Clarke and May[1] have defined a parameter by which the magnitude of these waves may be qualitatively described. This parameter is commonly referred to as the maximum initial reverse pressure difference, ΔP_i, calculated by subtracting the pressure near the base of the projectile from the gun breech pressure. Ideally this difference is positive or zero, and large negative values are indicative of poor propellant charge ignition and subsequent redistribution of the charge into void areas in the chamber.

Large negative values of ΔP_i are indicative of large pressure wave action that, amongst other problems, creates greater early-time transient projectile loading. Large impulsive loads to the projectile due to gas pressure, grain impact, and case closure plug impact have been measured in the presence of large-magnitude pressure waves. In the past, projectile in-bore and close aboard malfunctions have occured when there were significant chamber pressure waves such as reported in References 2 and 3. Futhermore, large negative values of ΔP_i have been recorded coincident with other instances of poor charge assembly performance that were caused by nonuniform ingition of the propellant bed. A gun malfunction reported in Reference 4 was attributed to a flow blockage in a base-ignited 76-mm OTO MELARA chage assembly resulting in restricted ignition, excessive pressure waves, and a very large negative value of ΔP_i. In fact, poor ignition has been correlated with excessive pressure waves in References 1 through 7, where excessive pressure waves have correlated with severe projectile loading. However, this study shows that transient projectile loading cannot always be correlated with pressure wave activity alone and that the initial loads transmitted by plug and propellant movement can create severe projectile shock conditions.

The data from four igniter development tests, which will be explained in detail later, demonstrate the lack of correlation between pressure waves

---

* Superscript numerals refer to identically numbered references listed at the end of the text.

and early-time transient projectile acceleration. These four tests were conducted to evaluate candidate igniter designs being considered for incorporation in a charge assembly for use with the 8-in. ERGP. The five igniter designs that were tested included a HIVELITE rapid ignition propagation (RIP), an aluminum potassium perchlorate (ALCLO) RIP, a black powder RIP (BP RIP), and a BP igniter. The RIP igniter concepts were investigated because of their ability to uniformly ignite the propellant bed and reduce pressure waves in the 5"/54 gun system. The afterbody configuration of the ERGP incorporated long trailing fins which extended 1.5 calibers into the gun chamber. The ullage around the fins, located between the front of the propellant bed and the base of the projectile, was approximately 20 percent of the total initial chamber volume. A large forward ullage in the gun chamber has previously been associated with traveling pressure waves and severe transient projectile accelerations.

The first of the four tests in this series was an open-air test to measure the axial propagation rate of the luminous flame front produced by each igniter. The second laboratory test was intended to characterize the time-dependent pressure distribution in an inert propellant bed. The third test was an actual gunfiring that was designed to compare the performance of five candidate igniters by measuring the pressure distribution in the chamber and the resulting early-time projectile loading during the interior ballistic event. A final test of a live propellant bed in the new 8-in. fiberglass disposable breech test fixture was designed to record charge assembly component movement, flame front spread, bed pressurization, and projectile response.

EXPERIMENTAL TECHNIQUE AND HARDWARE

Open-air and inert-bed tests were conducted to evaluate the performance characteristics of the five igniter configurations. The sole purpose of the open-air tests was to define the axial propagation rate of the flame front for each design for the pyrotechnic weights considered. The flame front propagation of the HIVELITE and ALCLO units was recorded using a HYCAM camera operating at a framing rate of 40,000-frames/sec. A 1/2-frame (8-mm) FASTEX camera with a 13,000-frames/sec framing rate was used to record the BP and BP RIP firings. In all tests, the igniter was fixed at its base in a section of a cartridge case so that the entire length of the igniter was visible to the camera.

The inert-bed test was conducted in a fixture that included an entire charge assembly containing an 8-in.-granulation inert propellant. A standard cartridge case was modified to include six pressure ports at 6.4, 23.6, 39.7, 56.5, 73.3, and 90.2 cm (2.5, 9.4, 15.6, 22.3, 28.9, and 35.5 in.) from the front of the lip of the case base. Kistler 202A1 pressure transducers with a linear range of 0 to 34.5 MPa (0 to 5 kpsi) were used to measure the internal case pressures. The case closure plug was held in place by the test fixture during pressurization to provide a pressure seal at the case mouth.

Actual gunfire tests were conducted in a simulated Major-Caliber Lightweight Gun (MCLWG) incorporating an 8"/51 Mk 29 instrumented barrel. The purpose

of these tests was to measure chamber sidewall pressures and projectile base acceleration. Pressure instrumentation in the chamber consisted of six Kistler 607A pressure transducers with a maximum linear range of 0 to 483 MPa (0 to 70 kpsi). Two transducers were mounted in the base of the cartridge case to record data at 5.7 cm (2.3 in.) from the breech face of the gun. The remaining four gauges were mounted on the chamber sidewall at 50.8, 77.0, 116.8, and 153.4 cm (20.0, 30.3, 46.0, and 60.4 in.) from the breech face. The tranducers located at 5.7 and 116.8 cm were at the extreme ends of the chamber as it existed after ramming, and the transducer at 153.4 cm was in front of the projectile obturator. Hence, it was possible to map the pressure distribution throughout the entire length of the chamber even after 22.1 cm (8.7 in.) of projectile travel.

The simulated ERGP used in the gunfiring test is shown in Figure 1. It consisted of the body and nose fuse of a standard 8-in. Mk 25 projectile, six simulated tailfins welded to a simulated tailfin hinge plate, a nylon obturator band, lead shot ballast, a steel instrumentation conduit, and an Endevco 2292 accelerometer. The ballast filled the explosive cavity in the projectile and brought the simulated ERGP up to the weight of the actual projectile. The Endevco 2292 accelerometer had a linear range of 0 to ±20 kg. That portion of the projectile aft of the obturator closely simulated the features of the ERGP significant to the interior ballistic event.

The five igniters tested consisted of two containing HIVELITE* 300435 pyrotechnic pellets, one containing ALCLO pyrotechnic pellets, and two containing BP. All but one of the designs, the BP igniter, incorporated a mild-detonating fuze (MDF) along the entire length of the igniter to ensure initiation of the pyrotechnic material at an axial rate of 6100 m/s (20,000 ft/sec). The two HIVELITE igniters differed only in the total energy content of the pyrotechnic material, 90 kcal (376.6 kJ) and 120 kcal (502 kJ). The pyrotechnic material was evenly spaced along the entire length of the Plexiglass tube as shown in Figure 2. The explosive train in the igniter was initiated by a bridge-wire/lead styphnate element, taken from a Mk 1 Mod 1 ignition element. Transition to the MDF was made via a 70-mg charge of lead azide and 70-mg charge of hexanitrostilbene (HNS) contained in a stainless-steel ignition element, Item 6 in Figure 2.

The ignition train used in the HIVELITE igniter was also used in the ALCLO and BP RIP igniters. The tube containing the pyrotechnic was the same length as the previous tube except it was 4130 seamless steel tubing containing vent holes along its entire length and was capped with a threaded steel closure. The ALCLO igniter contained 120 kcal (502 kJ) of energy in the pyrotechnic material and the BP RIP igniter contained 120 kcal (502 kJ) of energy in the BP load. A section view of the ALCLO design is given in Figure 3; however, the only difference between the igniter shown and the BP RIP was the pyrotechnic material. The BP igniter was a Mk 37 Mod 2 igniter with a 49.5-cm (19.5-in.) unvented length of steel tubing prior to the first vent hole. The BP igniter also contained 120 kcal (502 kJ) of energy in the BP load.

---

*Trademark of the Teledyne/McCormick Selph

The RIP igniters extended through the entire length of the propellant bed as shown in Figures 4 and 5. The external configuration of the ALCLO and BP RIP designs was identical. The BP igniter was 79.0 cm (31.1 in.) long and extended through approximately 80 percent of the propellant bed as shown in Figure 6.

The charge assembly utilized in these tests closely simulated the anticipated final design of the 8-in. ERGP charge, and it incorporated one of the igniters mentioned above. An experimental design ETHAFOAM* case closure plug with a density of 0.14 g/cm^3 (9 lbm/ft^3) was selected for these tests. The charge consisted of 31.75 kg (70 lbm) of NACO propellant, SPCF-11154, and the cartridge case was a modified Mk 1 Mod 3 brass case. A section view of the assembled charge is shown in Figures 4 through 6.

RESULTS

GUNFIRE TESTS

The open-air and inert-bed tests were conducted first, followed by the gunfire tests. In the gunfire tests it was observed that the magnitude of the measured early-time projectile response did not correlate with the degree of the overall chamber pressure wave action. The next logical step would have been to conduct tests in the new 8-in. disposable breech gun to relate the igniter performance to the charge assembly response producing the projectile loading. Since funding for this program had been suspended, the disposable breech gun tests could not be performed. The only recourse was to review the open-air and inert-bed test data characterizing the igniter performance in order to explain the lack of correlation between projectile loading and chamber pressure waves. The gunfire test results will be discussed first to demonstrate the lack of correlation. The laboratory test results will then be reviewed to identify the igniter performance characteristics deemed responsible for the projectile loading.

The interior ballistic data measured in the gunfire tests indicated that there was no correlation between the magnitude of the observed early-time transient accelerations and the magnitude of ΔP_i or dP/dt at the base of the projectile. This implied that the majority of the transient projectile response was due to mechanical impact on the base of the projectile. It is hypothesized that the mechanical impact was triggered by small amplitude pressure waves. Furthermore, the fact that ΔP_i occurred well after the maximum early-time loading also indicated that the gas pressure impulse did not contribute significantly to the transient projectile loading.

The round-to-round performance variations within each group of three identical igniters were small. In spite of the small round count in each group the data are complete and consistent enough to allow meaningful conclusions about the performance of each igniter. A summary of the pertinent interior ballistic data for the gunfire tests is presented in Tables 1 and 2. Table 1 lists

---

* Trademark of Dow Chemical

the data for all 15 rounds in the gunfire tests. Table 2 summarizes the average performance of each group of igniters in the open-air and inert-bed tests as well as in the gunfire tests.

Both HIVELITE igniter designs produced an average early-time projectile response that was approximately 40, 20, and 7 percent of that produced by the BP, ALCLO, and BP RIP igniters, respectively. The pressure wave action, as measured over the entire length of the chamber by ΔP_i, was essentially the same for all of the igniters, +3.5 to -11.7 MPa (+0.5 to -1.7 kpsi). The above indicators were consistent with the maximum rates of pressure rise measured at the projectile base, dP/dt, of 20,700 to 27,600 MPa/s (3.0×10^6 to 4.0×10^6 psi/sec). The relatively low temporal pressure gradients at the projectile base for each ignition stimuli indicated that the impulse to the projectile due to the gas pressure was not significant. Based on this information, one can conclude that in this situation neither ΔP_i nor dP/dt was indicative of the total early-time loading on the projectile.

Most important was the fact that in all 15 test rounds the maximum early-time loading of the projectile occurred prior to the time at which ΔP_i occurred. A typical example of this time relationship is shown in Figure 7 where the maximum early-time projectile loading occurred before the maximum negative value of ΔP_i. In this figure, the pressure at 5.7 cm (2.3 in.) from the breech face is referred to as P_1 and that at 116.8 cm (46.0 in.) as P_5. It should be noted that in round 4 the BP igniter first vented at the middle of the bed and pressure was initially discerned at that point nearly 2 ms prior to pressurization at P_1 or P_5, the extreme ends of the chamber. As a result, the initial projectile accelerometer response occurred after first pressurization in the bed but before appreciable pressurization at the ends of the chamber. Thus, propellant bed motion dominated the first projectile loading sequence.

The uniformity of the propellant bed pressurization was evident in the pressure distance plots in Figures 8 through 12. There were no large traveling compression waves being reflected from either end of the chamber. Furthermore, the rate of pressurization at the projectile base was gradual and uniform, and there were only subtle differences in the pressure histories for rounds fired with any of the igniter designs. The pressure data indicated that small spatial pressure gradients existed in the front one-third of the propellant bed during the first 3 ms of interior ballistic event. These gradients were produced by nonuniform ignition of the bed and probably resulted in compaction and translation of the forward portion of the bed. Depending on the magnitude of these gradients, they may have imparted substantial momentum to the compacted forwarded portion of the bed.

Figures 13 through 17 present projectile base acceleration histories that are representative of each of the five igniter designs. The accelerometer response was initially recorded as an analog signal and was low-pass-at 80 kHz. The analog record was then digitized at a sampling rate of 160 kHz to ensure against the introduction of aliasing errors in the subsequent frequency spectrum analysis. The fast Fourier transform (FFT) method was implemented to evaluate the relative level of high-frequency energy content associated with a given acceleration history. The excitation associated with the higher frequency components is considered

significant in view of sensitive small guidance and fuzing components of a guided projectile. The Fourier spectrum for each projectile response is shown above its corresponding acceleration history in Figures 13 through 17. As the forcing function on the base of the projectile approached a step function, the magnitudes of the high-frequency amplitudes increased relative to the zero-frequency amplitude. At frequencies greater than 10 kHz, the amplitudes relative to that of the zero frequency amplitude were much smaller for the HIVELITE igniters than the other three igniters. This fact was important in that it indicated a more gradually projectile loading when a HIVELITE igniter was used in comparison to a more impulsive loading of the projectile when other igniters were used.

Only the HIVELITE igniters were able to reduce the transient projectile response to a level equal to or below the rigid body design limits of the ERGP. Acceleration data were recorded for approximately 8 ms into the interior ballistic event. This time span corresponds to the first 30 percent of the interior ballistic event; i.e., a time interval that certainly included any significant early-time loading. The acceleration histories in Figures 15 through 17 for the BP, ALCLO, and BP RIP igniters indicate both set forward and setback loads in excess of the limits set for rigid-body acceleration. The Fourier spectra for these three rounds had greater high-frequency content indicating a higher degree of impact loading of the projectile than those for the HIVELITE igniters. Furthermore, the accelerations produced by the BP RIP igniter were recorded in excess of ±55 kg.

OPEN-AIR TESTS

Laboratory tests were conducted to compare the performance characteristics of each igniter. The data were re-evaluated after the gunfire test to help explain the observed projectile responses. Open-air igniter tests with high-speed color cinematographic coverage were performed to measure the axial and radial propagation rates of the luminous flame front. A representative record for each of the five types of igniters is presented in Figures 18 through 22. The framing rate for the HIVELITE and ALCLO igniter test records shown in Figures 18, 19, and 21 was approximately 40,000 frames/sec. A framing rate of 13,000 frames/sec was used for the BP and BP RIP igniter test records shown in Figures 20 and 22.

Average propagation rates of the luminous flame are tabulated in Table 2. Note that the HIVELITE igniter has an axial propagation rate five to eight times greater than that of the other designs. The propagation time of the MDF was not included in computation of the propagation rate of any of the igniters since it was assumed that the energy input to the bed by the MDF was small relative to that by the pyrotechnic material. The propagation of the MDF in Figure 18 was visible as a bright light ahead of the more voluminous, less intense HIVELITE plume, both advancing at approximately the same rate, 6100 m/s (20,000 ft/sec). Even though the axial propagation rate of the igniter was more significant, it was important to note that the HIVELITE igniter's radial propagation rate was two to four times greater than that of the other igniters. Furthermore, there appeared to be less variability from round to round with the HIVELITE igniters

than with the other igniters. Analysis of the propagation of the HIVELITE flame front in the open air indicated that this igniter should ignite the bed more uniformly, in time and space, and more reproducibly than the other igniters tested.

The BP igniter introduced its energy into a torus surrounding the first few vent holes of the steel igniter tube and then later at the top of the igniter where some of the BP was expelled from the end of the tube. The cinematographic coverage such as in Figure 20 indicated that the BP igniter provided centralized bed ignition resulting in pressure waves which would reflect from both ends of the chamber. The propagation rate of the BP igniter was much slower than that of the HIVELITE igniters. The ALCLO igniter performance, as recorded in Figure 21, was characterized by an axial propagation rate of 670 m/s (2,200 ft/sec) and a variability in the flame front propagation. On one occasion it propagated primarily from the base and on another occasion from both ends. An example of the latter is shown in Figure 21. The propagation of the flame front for the BP RIP igniter was much slower than for the HIVELITE igniter. As shown in Figure 22, the BP RIP igniter outgassing did not exhibit circumferential symmetry and the radial expansion of the plume was much slower than for the other designs.

INERT PROPELLANT BED TESTS

Inert propellant bed tests were conducted to determine the uniformity of the bed pressurization, to make a qualitative determination of the times required for the igniters to introduce their energy into the propellant bed and to ascertain the maximum chamber pressure generated by the igniters. The pressurization time was considered a qualitative indicator of the time required for the igniter to supply its energy to the bed and to ignite a live propellant bed. Second, the peak bed pressure was considered a qualitative measure of the igniter's ability to create a uniform pressurized environment conducive to a reproducible self-sustaining bed reaction. Other subjective evaluations were made concerning criteria such as uniformity and repeatability of the ignition stimuli.

The HIVELITE igniter was superior to the other igniters considering all the above performance criteria. Representative time-dependent pressure distributions for each igniter in an inert bed are presented in Figures 23 through 27. A summary of the average performance parameters for each of the three-round groups for each igniter is included in Table 2. The HIVELITE igniters produced a peak bed pressure in 0.48 to 0.68 ms in comparison with 1.30, 1.50, and 1.50 ms for the BP, ALCLO, and BP RIP igniters. As shown in Figures 23 and 24, the pressure distributions at peak pressure were much more uniform than those for the other igniters at comparable times. The low pressures at the case mouth in Figures 23 and 27 was due to leakage past the case closure plug. The pressures in Figure 25 supported the hypothesis that the BP primer ignited the bed in the vicinity of the first few vent holes of the BP primer and then later at the end of the igniter tube. The ALCLO igniter, as shown in Figure 26, pressurized the bed from both ends with pressure waves moving to the center of the charge. The time to peak pressure was approximately 1.6 ms. Of the other two rounds of ALCLO igniters fired in this group, one pressurized the bed primarily from

the base end while the other began near the case mouth. In both instances, spatial pressure gradients were set up in the front one-third of the propellant bed; a condition that could have caused significant forward grain motion in a live propellant bed. The last igniter design tested in the inert bed. Representative results are shown in Figure 27. The peak bed pressure was on the order of that produced by the HIVELITE igniter; however, the BP RIP igniter took much longer to introduce all of its energy into the bed. Another BP RIP igniter pressurized the bed from the base of the charge.

SUMMARY

Large-magnitude chamber pressure waves have previously been linked to severe early-time projectile accelerations because of a significant gas pressure contribution to the impulsive load on the base of the projectile. However, it was demonstrated here that, even in the absence of a large gas pressure impulse, the forward motion of the propellant bed and the plug imparted a severe impact load to the projectile. All of the charges that were ignited with the five igniters produced minimal pressure wave motion in the chamber. The magnitude of ΔP_i was small; the pressure component of the total impulse was not significant. However, only the two HIVELITE igniter designs ignited the bed in such a manner as to reduce significantly the overall projectile loading.

It was not possible to correlate the ΔP_i observed in the gunfire tests with the magnitude of the corresponding projectile early-time accelerations. The differences in ΔP_i among the various igniter designs were of the same magnitude as the maximum expected error in the pressure transducer responses. Hence, it was not possible to discriminate between the various average ΔP_is. However, an order of magnitude difference in the measured projectile response was recorded in the gunfire test. Projectile accelerometer response for the BP RIP ignited charges were an order of magnitude greater than for the HIVELITE ignited charges.

The more uniform ignition of the bed by the HIVELITE igniters lessened the pressure gradients in the forward portion of the bed near the projectile base. Analysis of high-speed cinematography taken during the open-air tests and pressure data recorded in the inert-bed tests showed that the BP, ALCLO, and BP RIP designs had significantly slower axial propagation rates than the HIVELITE designs. It was also determined that the HIVELITE igniters performed more repeatably from round to round than did the other igniters. The inert-bed tests confirmed the presence of a more uniform pressurization of the propellant bed of the HIVELITE igniter implying a more uniform ignition of the bed.

CONCLUSIONS AND RECOMMENDATIONS

The following conclusions were drawn from the laboratory and gunfire tests that were conducted to evaluate the five candidate igniters designed for use in the 8-in. ERGP's gun propelling charge assembly. The data reported pertains directly to the 8-in. ERGP fired from the MCLWG, but the general conclusions drawn from the data may apply to other projectile/charge assembly combinations.

a. An igniter cannot be evaluated solely on the basis of its ability to minimize traveling pressure waves in the chamber. The resultant early-time projectile loading must also be measured and considered prior to the selection of an igniter. The indicator of gross pressure wave motion in the chamber, ΔP_i, does not always correlate with the magnitude of the early-time projectile accelerations. The values of dP/dt at the projectile base and ΔP_i are indicative of the magnitude of the impulse due to gas pressure, however, not of the impulse attributed to propellant grain and plug impact. In this particular charge assembly/projectile combination, the early-time loading occurred well before the occurrence of ΔP_i. The response of an accelerometer mounted in the projectile base is a more direct indication of overall projectile loading than ΔP_i and dP/dt. Another indicator of the projectile loading may be the spatial pressure gradients in the front of the propellant bed during the first several milliseconds of the interior ballistics event. This gradient should be indicative of propellant bed compaction and motion that could result in a significant solid-particle impulsive loading.

b. The HIVELITE igniter produced lower-magnitude early-time projectile loading than the BP, ALCLO, and BP RIP igniters. The early-time average measured projectile base accelerometer response produced by the HIVELITE-ignited propelling charges was from 7 to 40 percent of that produced when other igniter designs were used to ignite the propelling charges. The difference in loading was attributed to the uniformity of the bed ignition, with respect to time and space, produced by the HIVELITE igniter. A proposed explanation of the higher accelerations with the other igniters was plug and propellant grain impact on the projectile base due to the pressure gradients in the front of the bed.

Should funding become available, laboratory tests similar to those reported by East, et al., in References 8 and 9 will be conducted in the new 8-in. disposable fiberglass breech simulator. These tests would provide time-correlated data concerning the reaction of the charge assembly to the various types of igniters and the subsequent projectile response. It would then be possible to directly relate igniter performance to charge assembly response and subsequent projectile loading.

REFERENCES

1. E. V. Clarke, Jr. and I. W. May, "Subtle Effects of Low-Amplitude Pressure Wave Dynamics on the Ballistic Performance of Guns," *11th JANNAF Combustion Meeting Proceedings*, Chemical Propulsion Information Agency, Johns Hopkins University, Applied Physics Laboratory, CPIA Publication 261, Baltimore, MD, December 1974.

2. M. C. Shamblen and J. S. O'Brasky, *Investigation of 8"/55 Close Aboard Malfunctions*, NWL TR-2753, Naval Surface Weapons Center, Dahlgren, VA, April 1973.

3. D. W. Culbertson, M. C. Shamblen, and J. S. O'Brasky, *Investigation of 5" Gun In-Bore Ammunition Malfunctions*, NWL TR-2624, Naval Surface Weapons Center, Dahlgren, VA, December 1971.

4. P. J. Olenick, Jr., *Investigation of the 76mm/62 Caliber MARK 75 Gun Mount Malfunction*, NSWC/DL TR-3144, Naval Surface Weapons Center, Dahlgren, VA, October 1975.

5. S. E. Hedden and G. A. Nance, *An Experimental Study of Pressure Waves in Gun Chambers*, NPG Report No. 1534, Naval Surface Weapons Center, Dahlgren, VA, 25 April 1957.

6. Chemical Propulsion Information Agency, "The Role of Ignition and Combustion in Gun Propulsion: A Survey of Developmental Efforts," *13th JANNAF Combustion Meeting Proceedings*, Combustion Work Group Committee on Gun Propellant Ignition and Combustion, Johns Hopkins University, Applied Physics Laboratory, Baltimore, MD, CPIA Publication 281, Vol. I, September 1976.

7. W. G. Soper, "Ignition Waves in Gun Chambers," *Combustion and Flame*, Vol. 20, pp. 157-162, 1973.

8. W. R. Burrell and J. L. East, Jr., *Effects of Production Packing Depth and Ignition Techniques on Propelling Charge Reaction and Projectile Response*, NSWC/DL TR-3705, Naval Surface Weapons Center, Dahlgren, VA, April 1978.

9. D. R. McClure and J. L. East, Jr., "Experimental Techniques for Investigating the Start-Up Ignition/Combustion Transients in Full-Scale Charge Assemblies," *11th JANNAF Combustion Meeting Proceedings*, Chemical Propulsion Information Agency, Johns Hopkins University, Applied Physics Laboratory, CPIA Publication 261, Baltimore, MD, December 1974.

Table 1. 8-in. Igniter Gunfire Test Results

Igniter	Calorific Content (kcal)	Round No.	Average Peak Chamber Pressure (kpsi)	Δp_i (kpsi)	Maximum $\Delta p/\Delta t$* (psi/sec)	Muzzle Velocity (ft/sec)	Maximum Early-Time Acceleration (kg)	
							Setback	Setforward
HIVELITE	120	8	29.0	-1.0	4.0×10^6	1982	+4.3	-3.0
		9	29.0	-1.2	4.0×10^6	1984	+4.6	-3.3
		10	29.0	-1.7	4.0×10^6	1982	+3.2	-3.5
HIVELITE	90	5	26.0	-2.0	4.0×10^6	1952	+2.2	-1.9
		6	25.5	-1.0	4.0×10^6	1952	+2.0	-2.5
		7	26.5	-2.0	3.0×10^6	1946	+5.9	-3.1
BP	120	2	28.5	+0.5	4.0×10^6	1961	--	--
		3	27.0	--	--	1942	+7.5	-13.2
		4	28.0	--	--	1944	+10.6	-20.5
ALCLO	120	11	27.0	-0.7	4.0×10^6	1926	+17.1	-7.5
		12	27.5	-1.3	3.0×10^6	1928	+32.2	-32.3
		13	28.0	-0.7	5.0×10^6	1924	+18.3	-22.7
BP RIP	120	14	27.5	-1.7	3.0×10^6	1945	+69.3	-56.8
		15	27.5	-1.0	3.0×10^6	1940	+48.2	-53.8
		16	28.0	-1.2	3.0×10^6	1943	--	--

*Measured at the projectile base, 116.8 cm (46.0 in.) from the breech face.

1 kcal = 4 184.0 kJ
1 psi/sec = 6 894.757 Pa/s
1 ft/sec = 0.3048 m/s

Table 2. Performance Characteristics of Candidate Igniters

Igniter	Pyrotechnic Energy Content (kcal)	Open-Air Test Ignition Propagation Rates		Inert-Bed Test			Maximum Early-Time Transient Load (kg)	ΔP_1 MPa (kpsi)	Maximum $\Delta P/\Delta t$ at Projectile Base (psi/sec)
		Axial (ft/sec)	Radial (ft/sec)	Time to Peak Pressure (ms)	Peak Pressure (psi)	Uniformity of Bed Pressurization			
HIVELITE	120	19,000	2,800	0.48	280	Uniform	+4.0/-3.3	-1.3	4.0×10^6
HIVELITE	90	16,000	2,500	0.68	210	Uniform	+3.4/-2.5	-1.7	3.7×10^6
BP	120	--	1,200	1.50	800*	Localized Ignition	+9.1/-16.5	+0.5	4.0×10^6
ALCLO	120	2,200	1,300	1.50	190	2 Points of Ignition	+22.5/-20.8	-0.9	4.0×10^6
BP RIP	120	2,900	650	1.30	280	Uniform	>+59.7/>-55.2	-1.3	3.0×10^6

* Localized about the first vent hole.

1 kcal = 4 184.0 kJ
1 ft/sec = 0.3048 m/s
1 psi/sec = 6 894.757 Pa/s

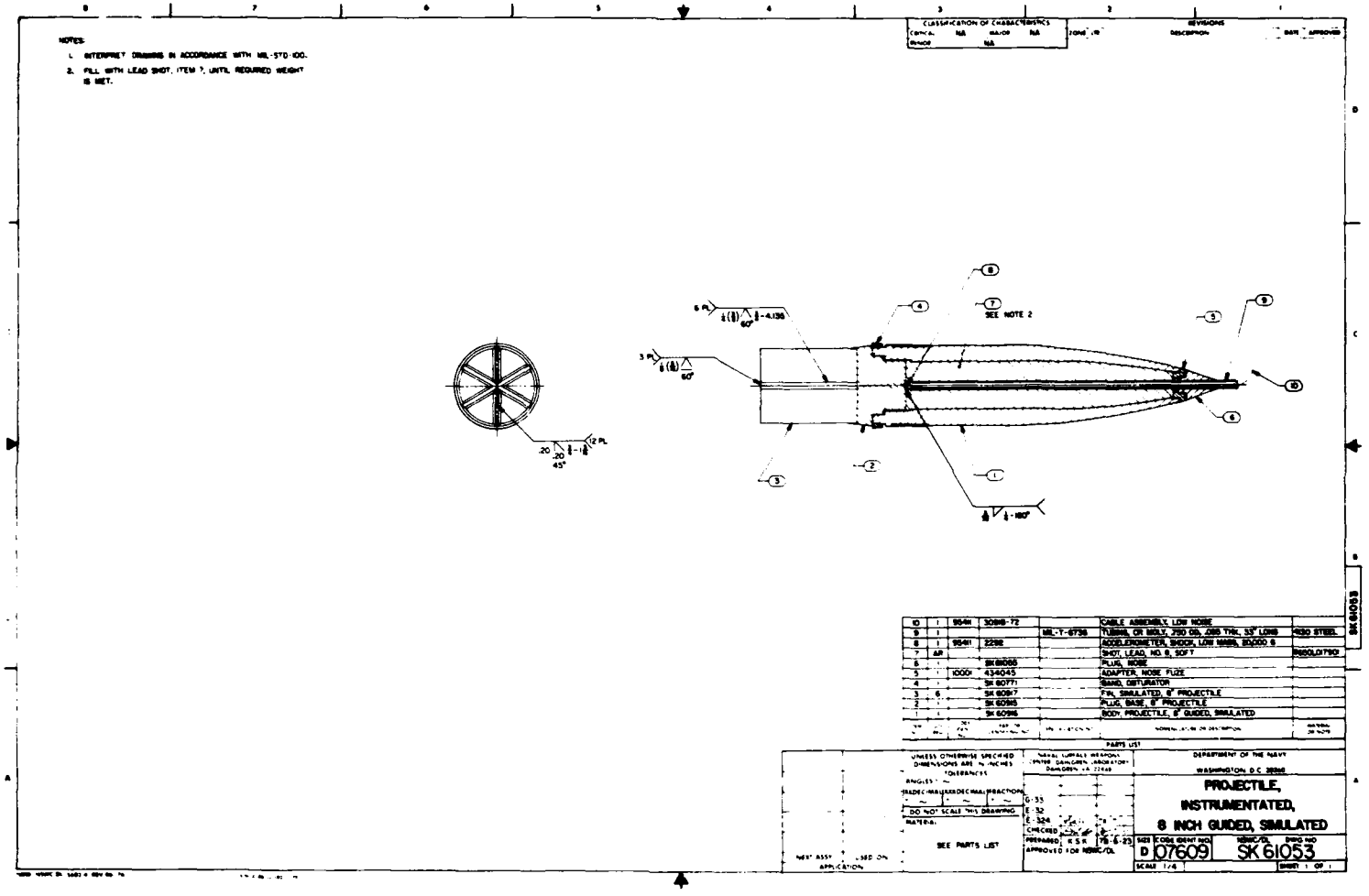

Figure 1. Simulated 8-in. Extended-Range Guided Projectile (ERGP)

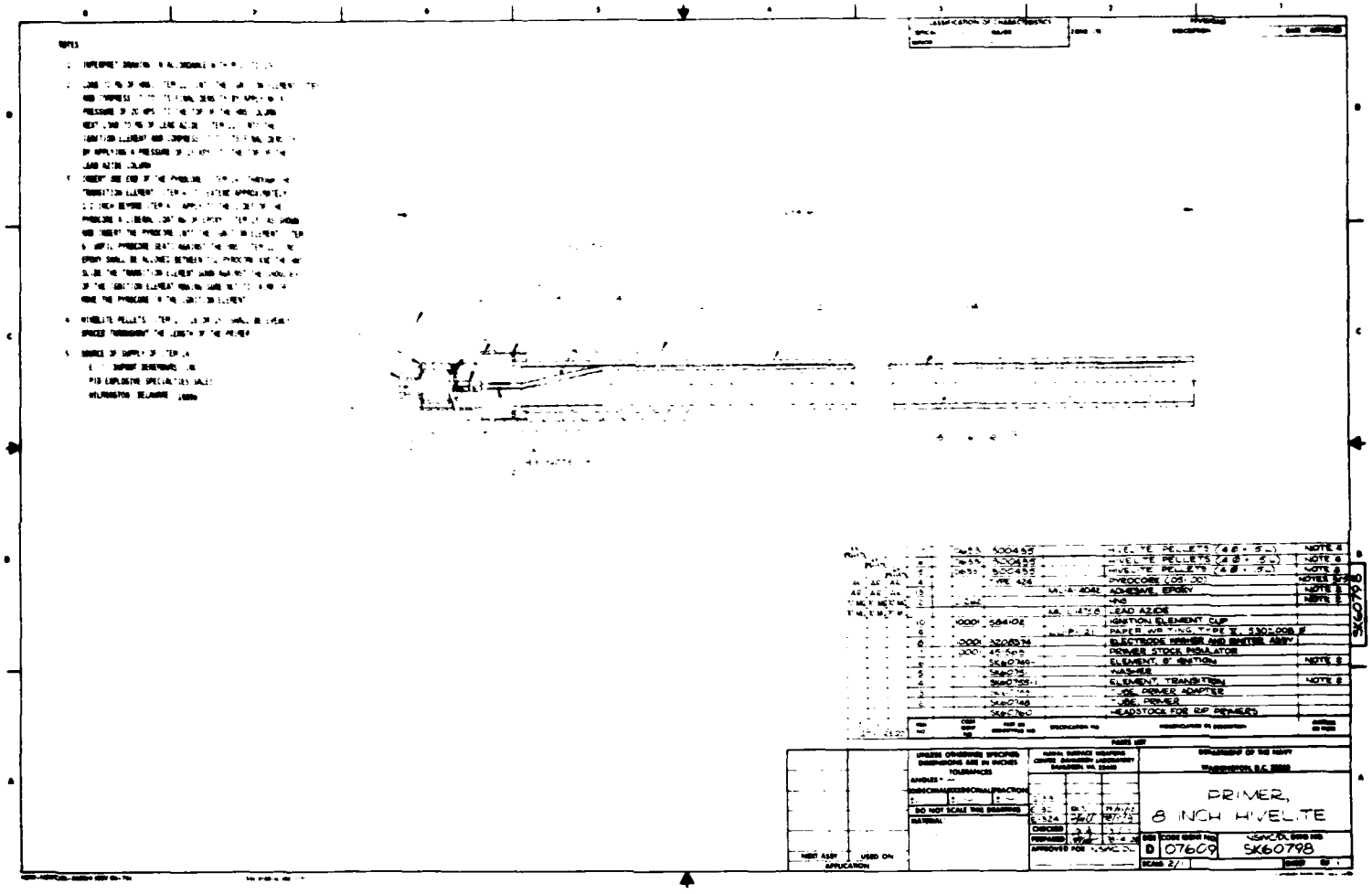

Figure 2. HIVELITE RIP Igniter

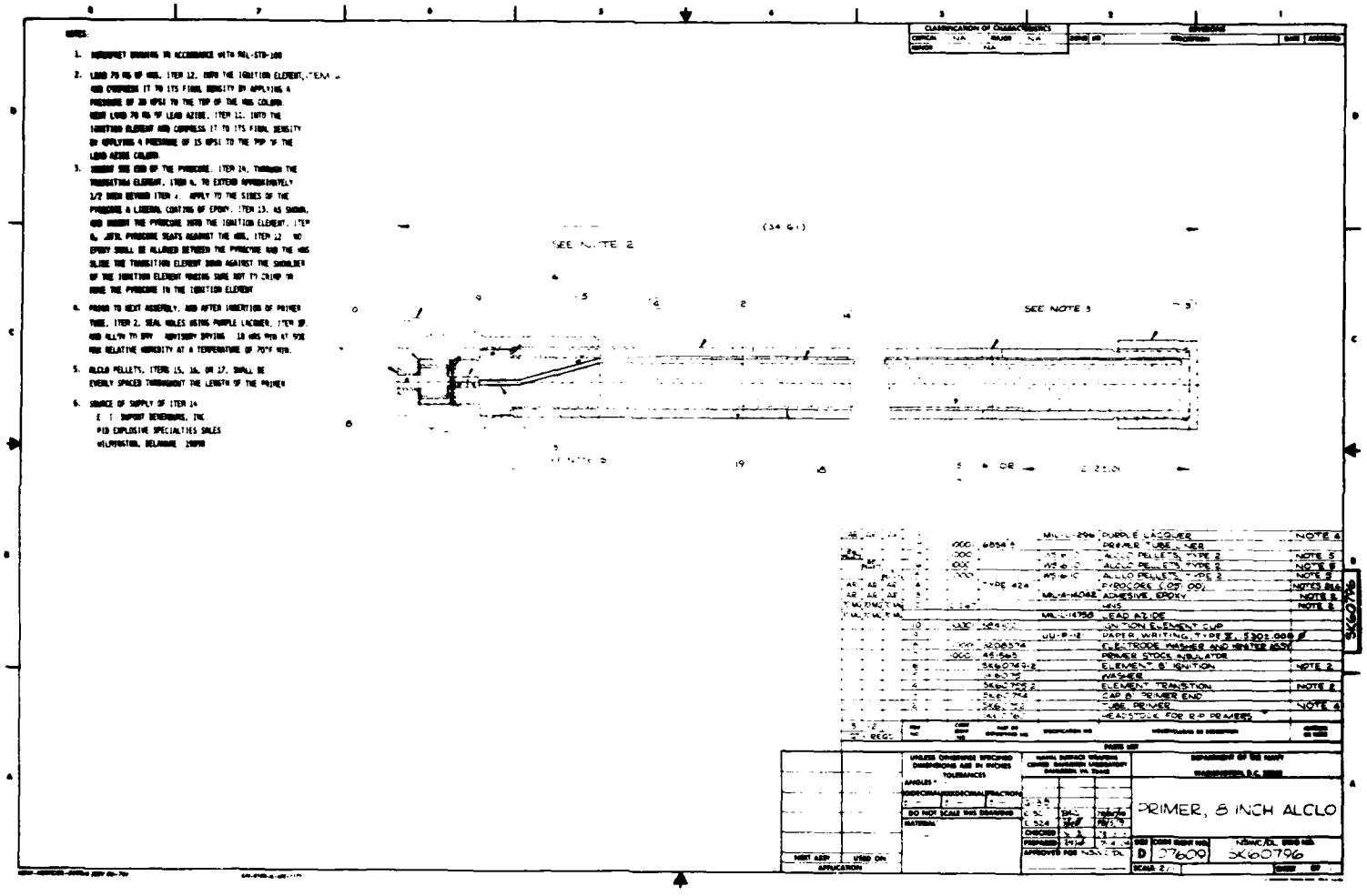

Figure 3. ALCLO RIP Igniter

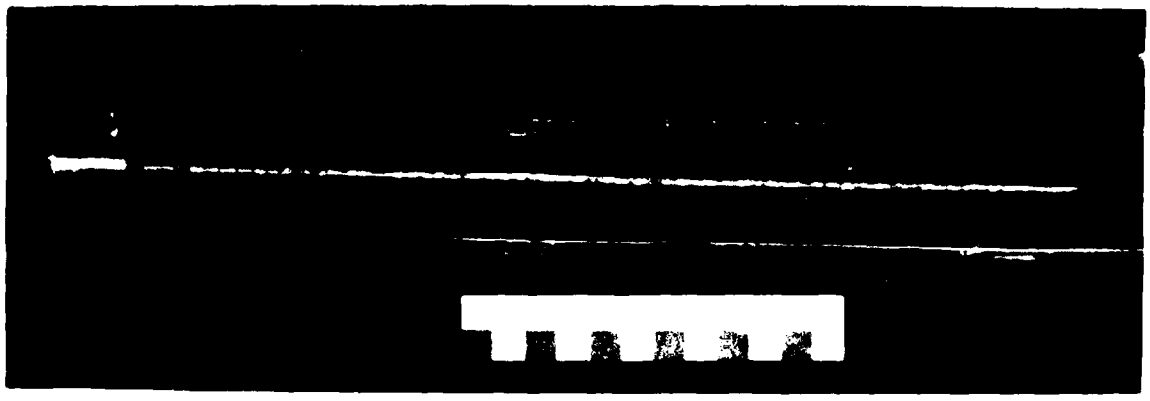

Figure 4. Charge Assembly with a HIVELITE Igniter

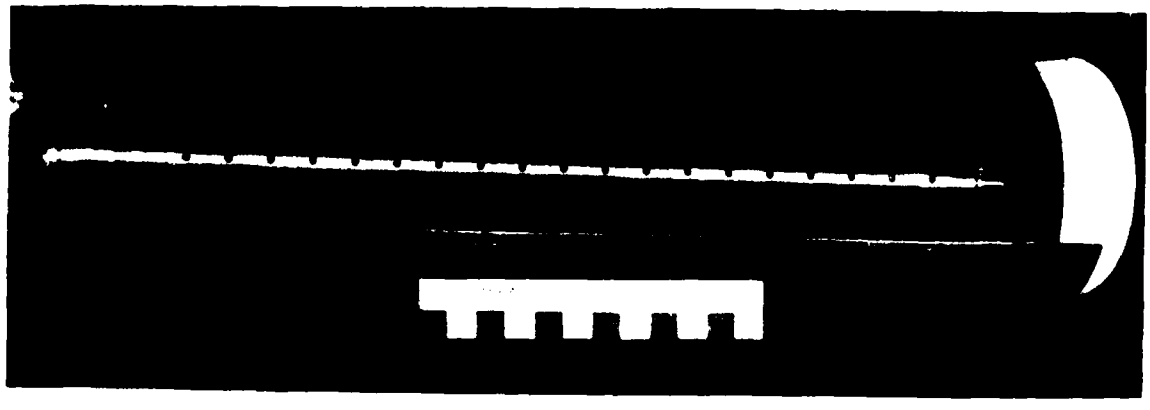

Figure 5. Charge Assembly with an ALCLO or BP RIP Igniter

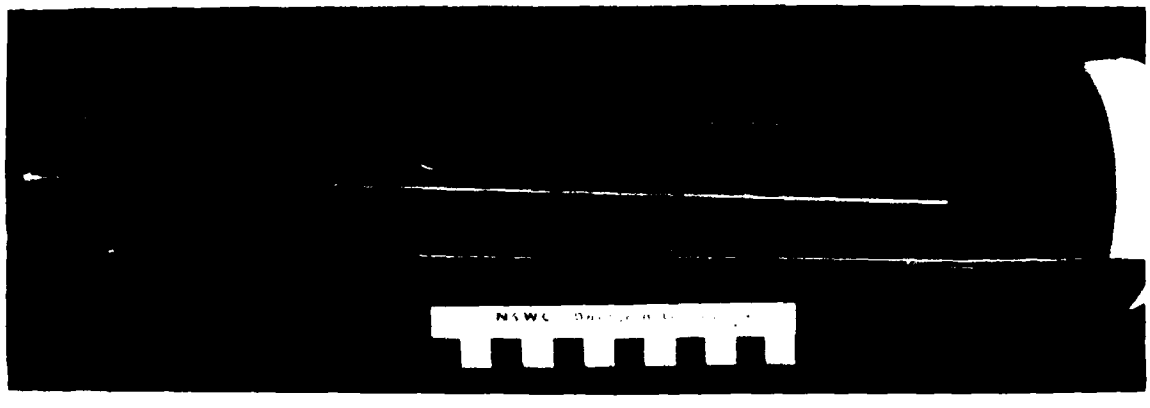

Figure 6. Charge Assembly with a BP Igniter

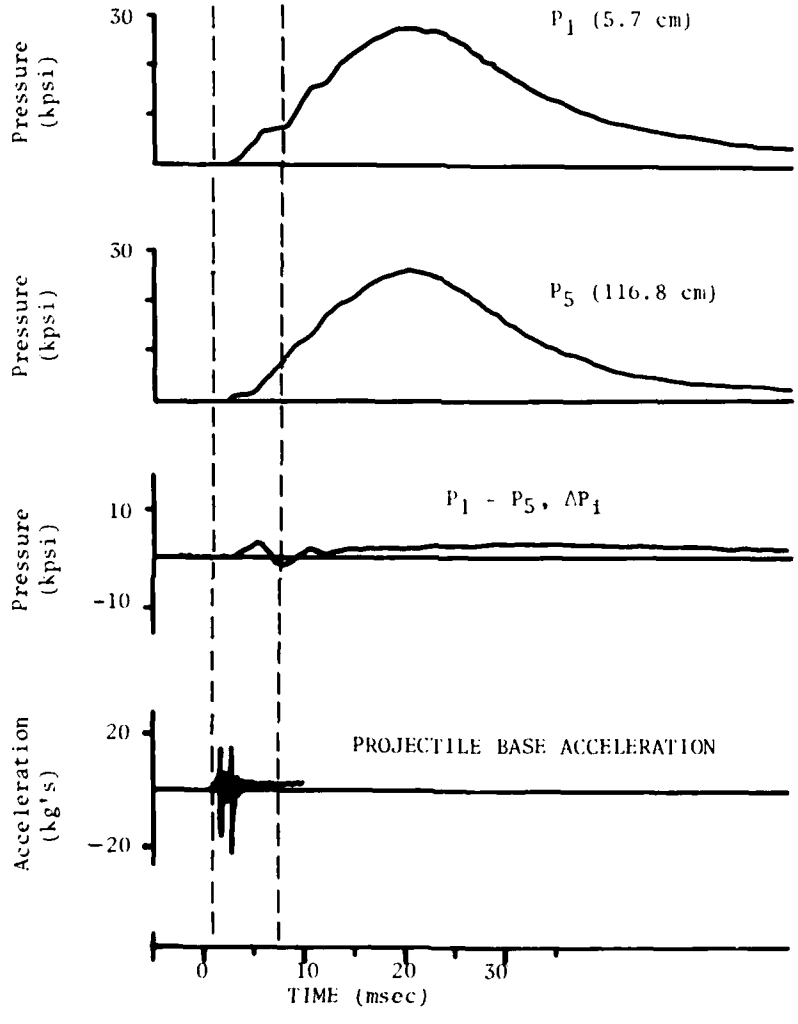

Figure 7. Time-Correlated Interior Ballistic Data for Round 4, BP Igniter

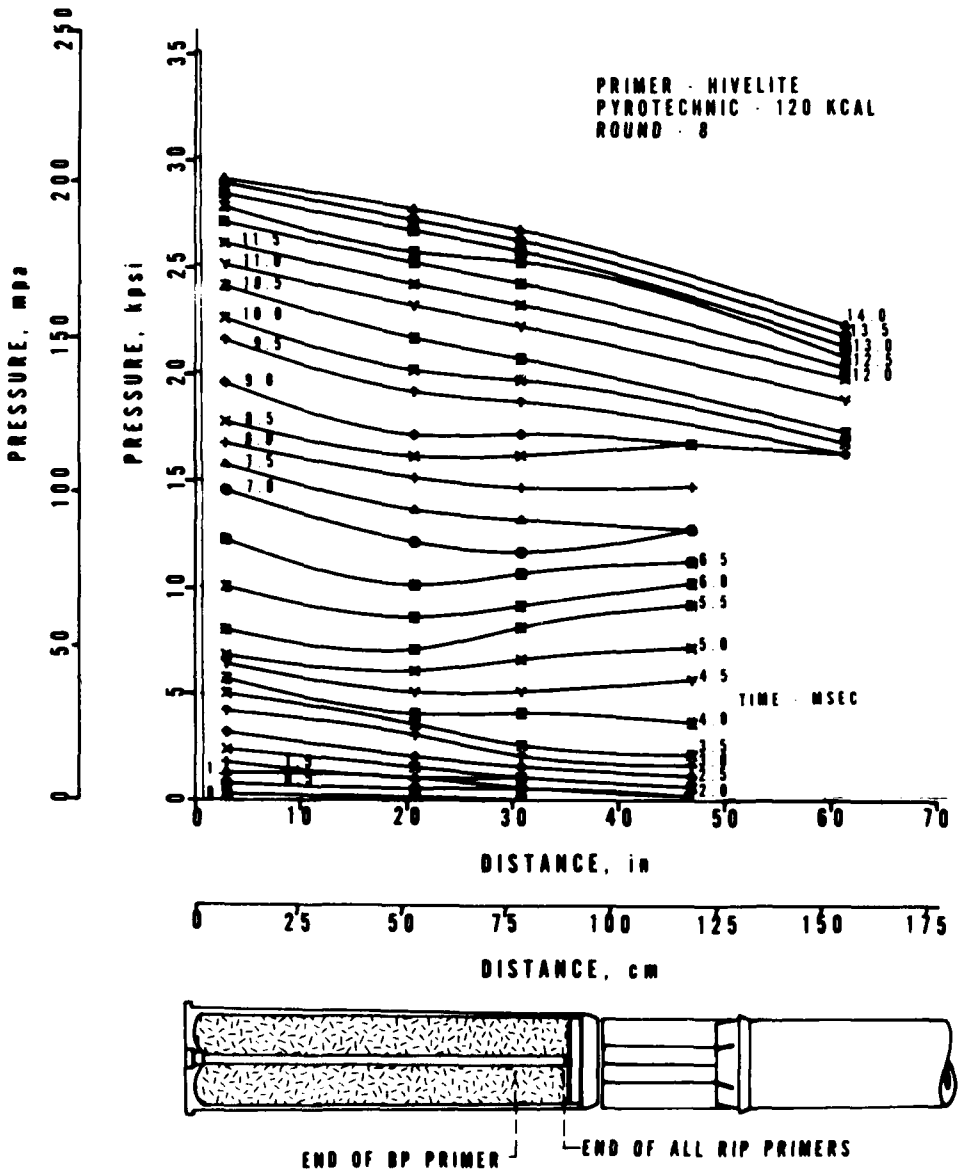

Figure 8. Chamber Pressure Distribution in Round 8, HIVELITE (120 kcal) Igniter

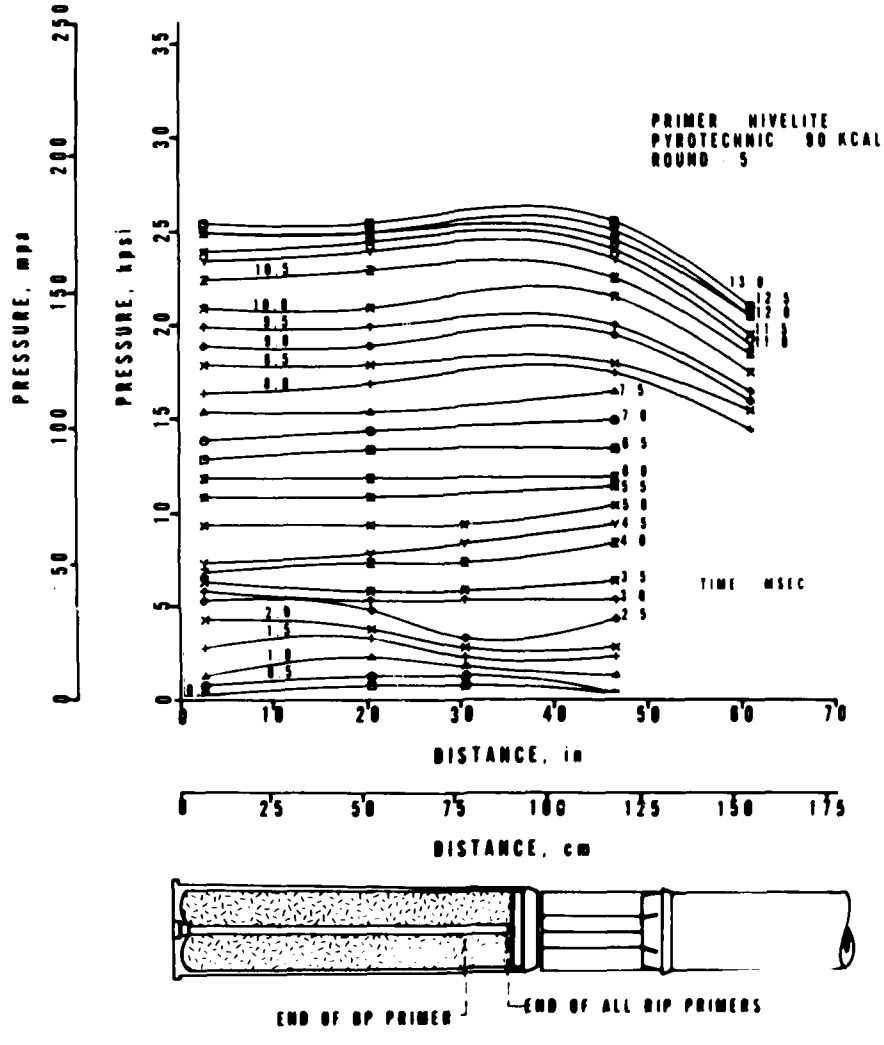

Figure 9. Chamber Pressure Distribution in Round 5, HIVELITE (90 kcal) Igniter

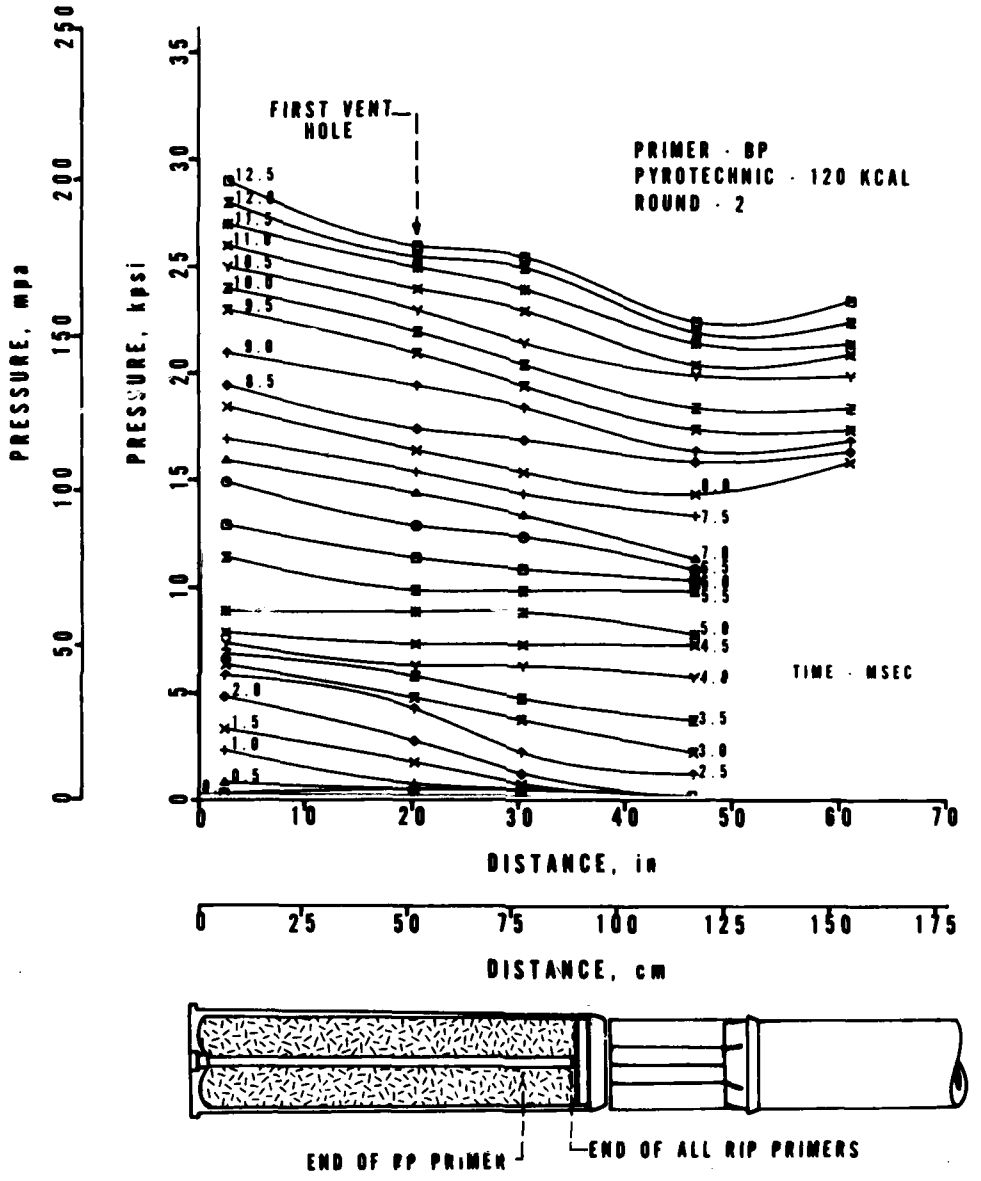

Figure 10. Chamber Pressure Distribution in Round 2, BP Igniter

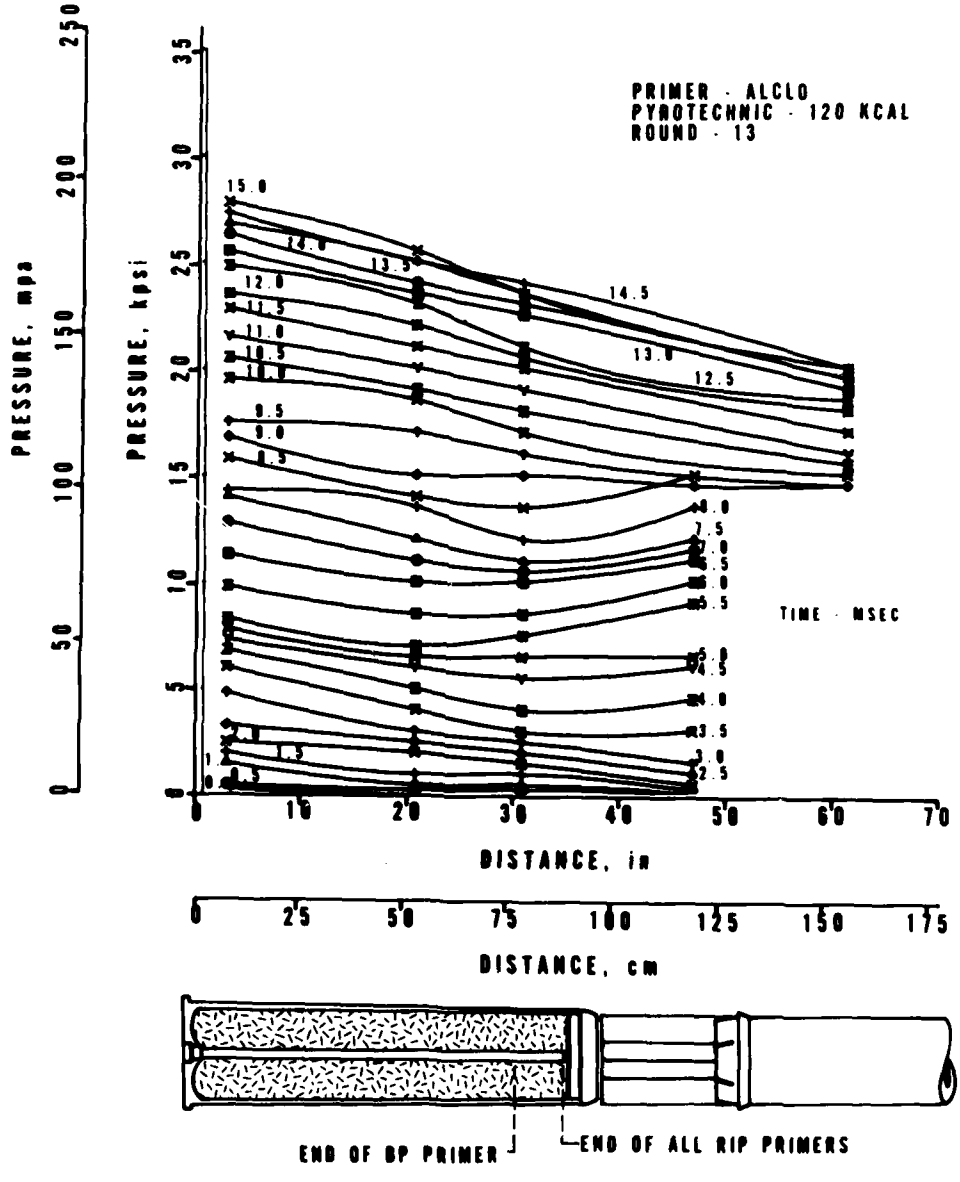

Figure 11. Chamber Pressure Distribution in Round 13, ALCLO Igniter

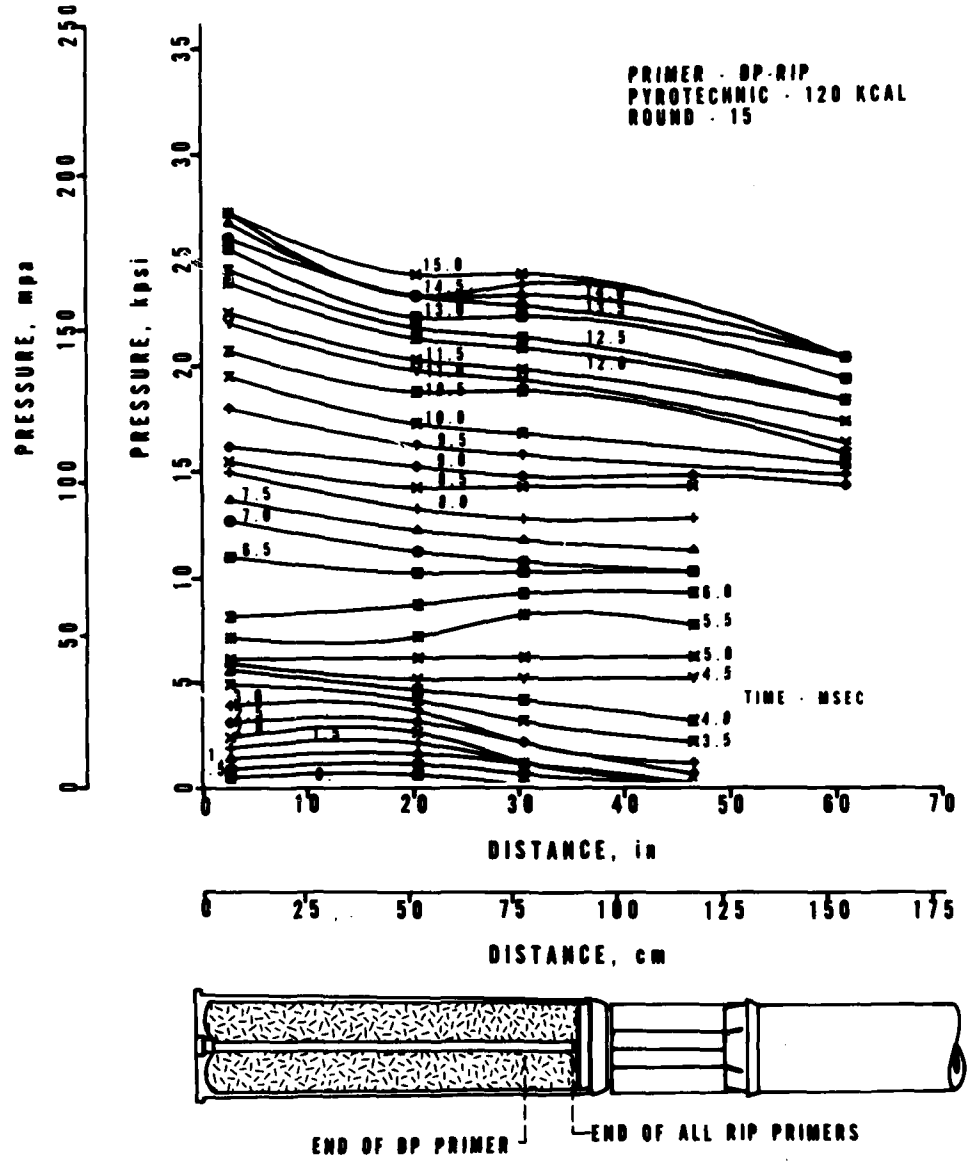

Figure 12. Chamber Pressure Distribution in Round 15, BP RIP Igniter

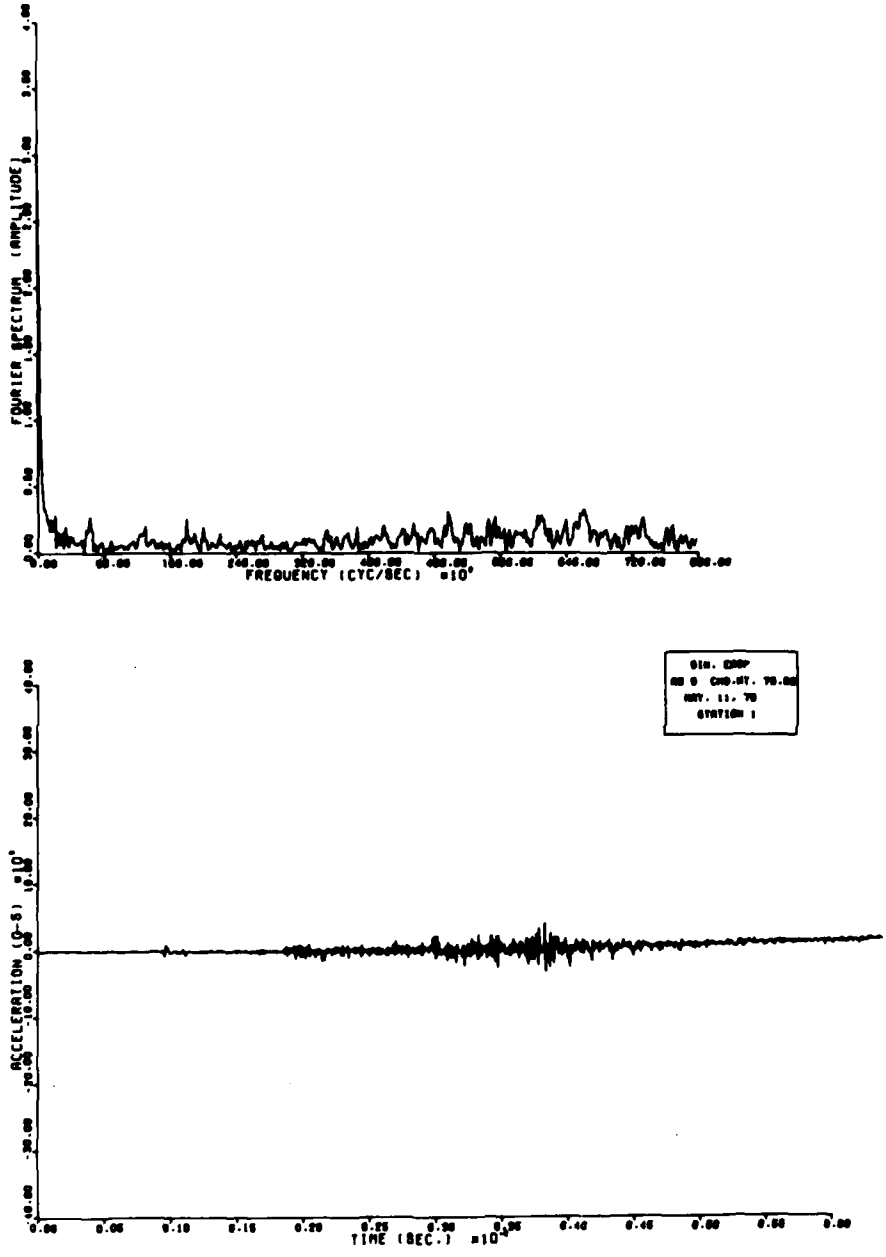

Figure 13. Fourier Spectrum and Corresponding Acceleration History, HIVELITE (120 kcal) Igniter

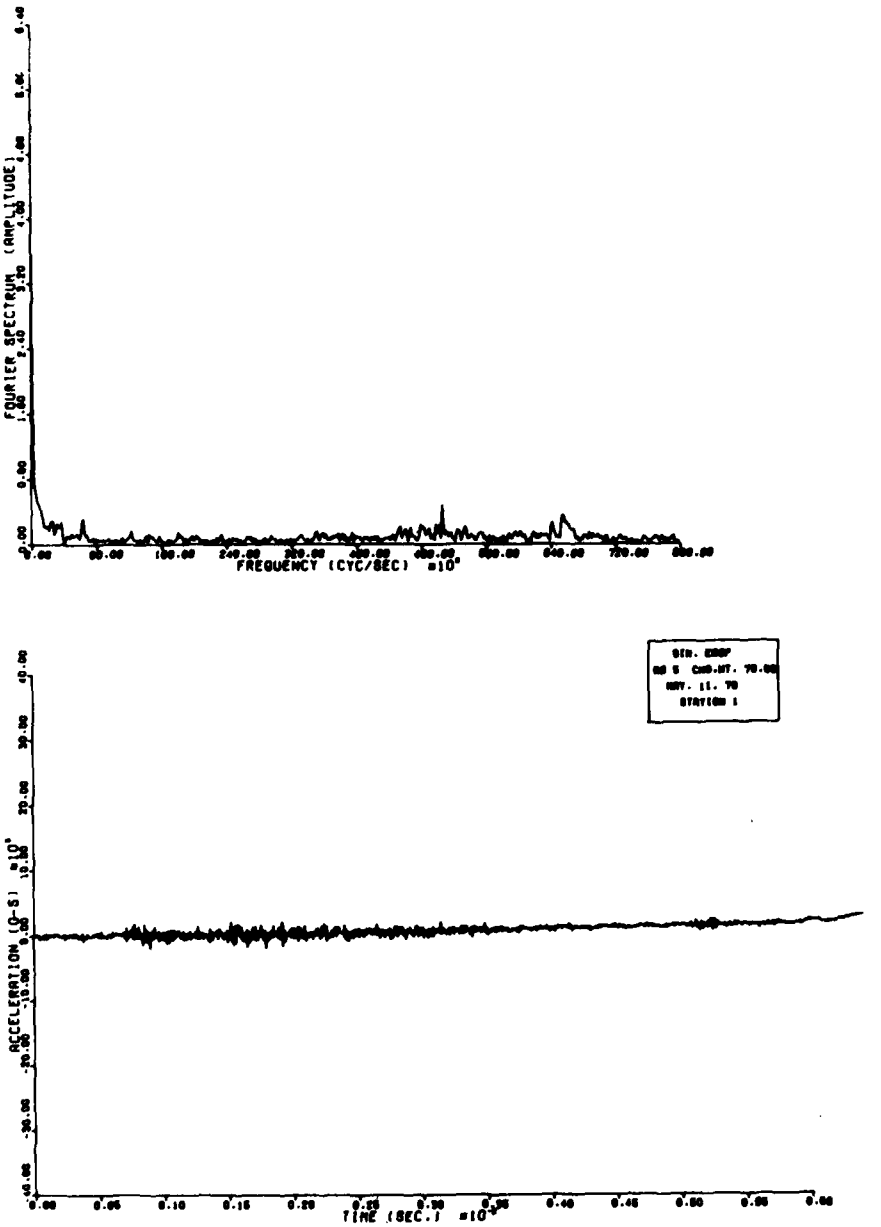

Figure 14. Fourier Spectrum and Corresponding Acceleration History, HIVELITE (90 kcal) Igniter

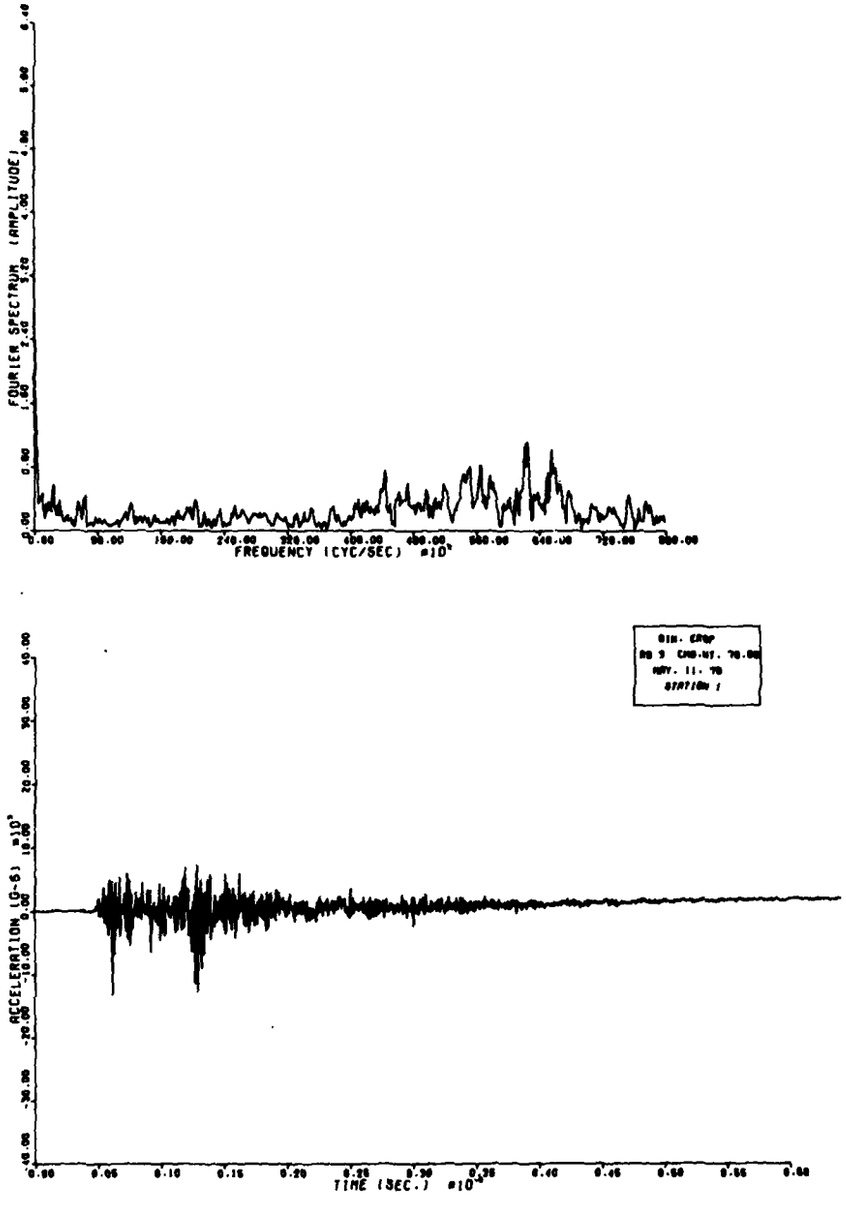

Figure 15. Fourier Spectrum and Corresponding Acceleration History, BP Igniter

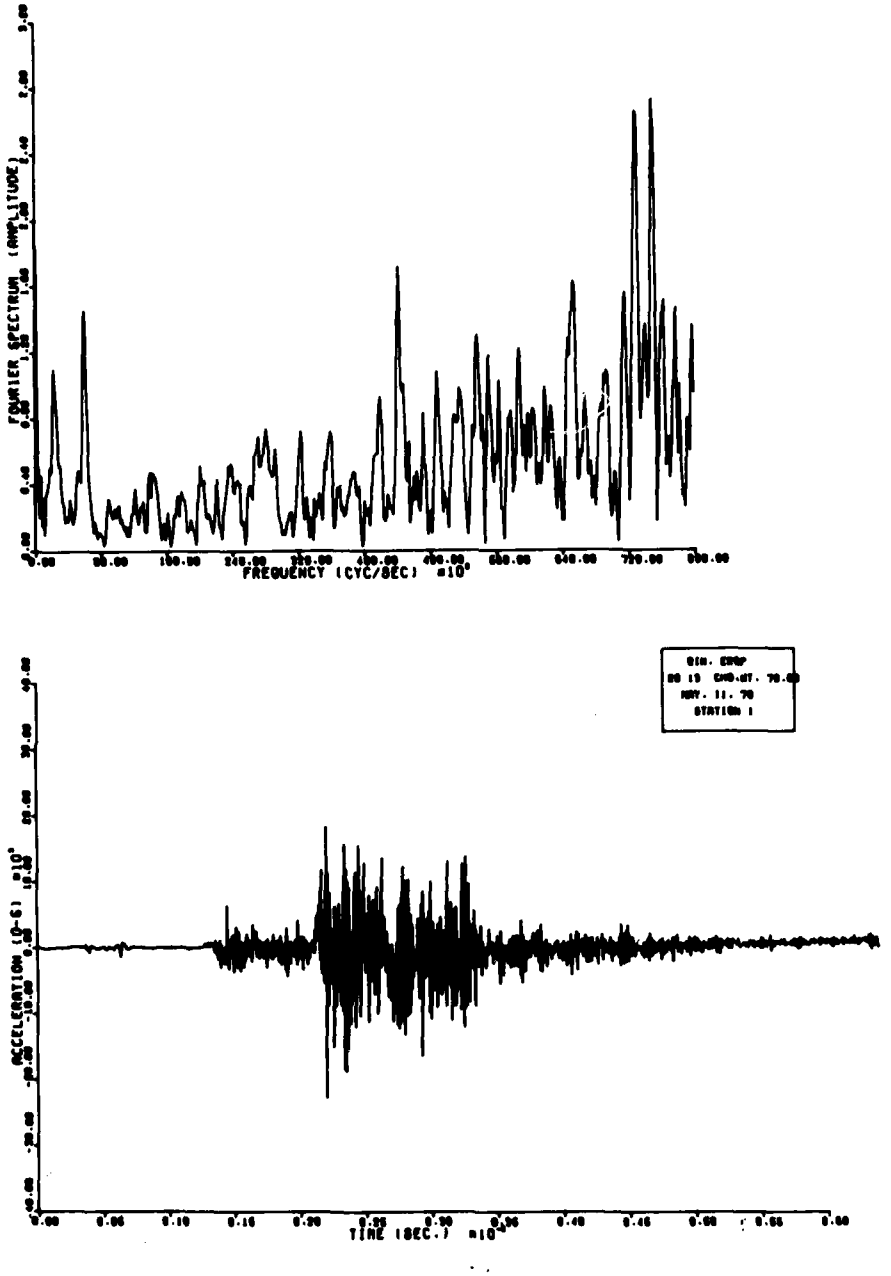

Figure 16. Fourier Spectrum and Corresponding Acceleration History, ALCLO Igniter

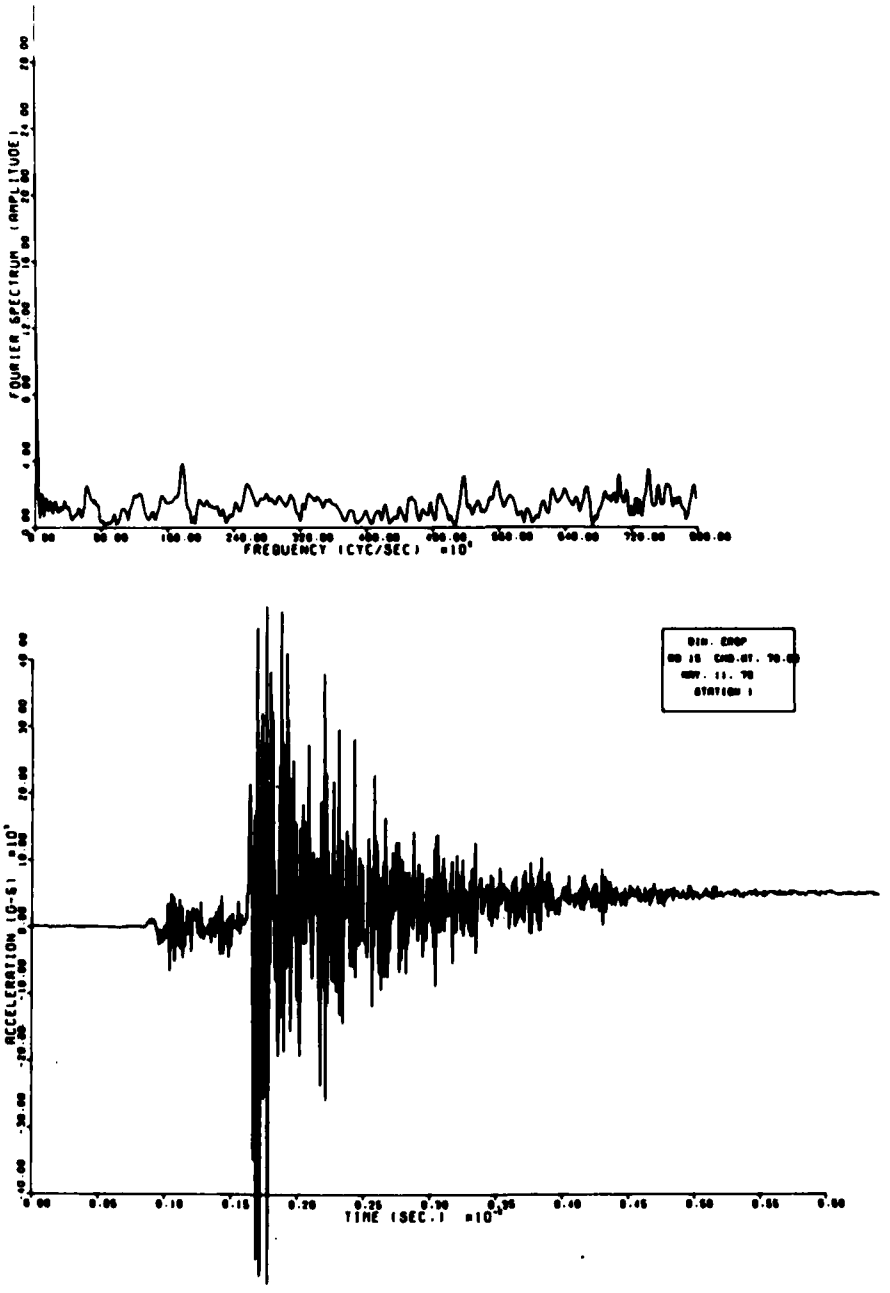

Figure 17. Fourier Spectrum and Corresponding Acceleration History, BP RIP Igniter

Figure 18. Propagation of the Luminous Flame Front, HIVELITE (120 kcal) Igniter

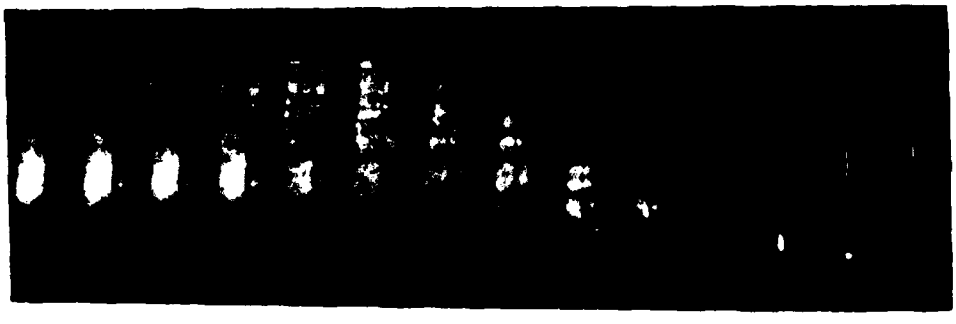

Figure 19. Propagation of the Luminous Flame Front, HIVELITE (90 kcal) Igniter

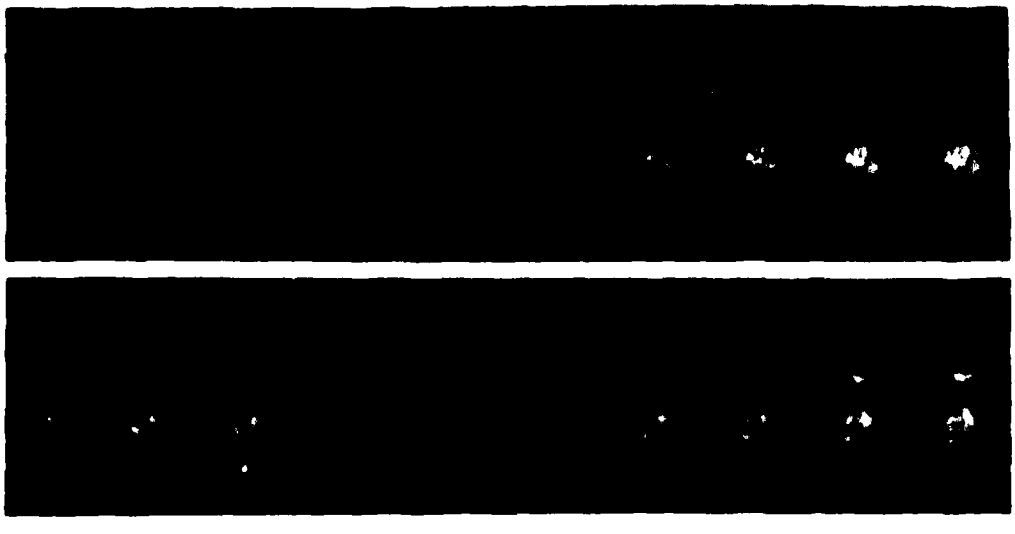

Figure 20. Propagation of the Luminous Flame Front, BP Igniter

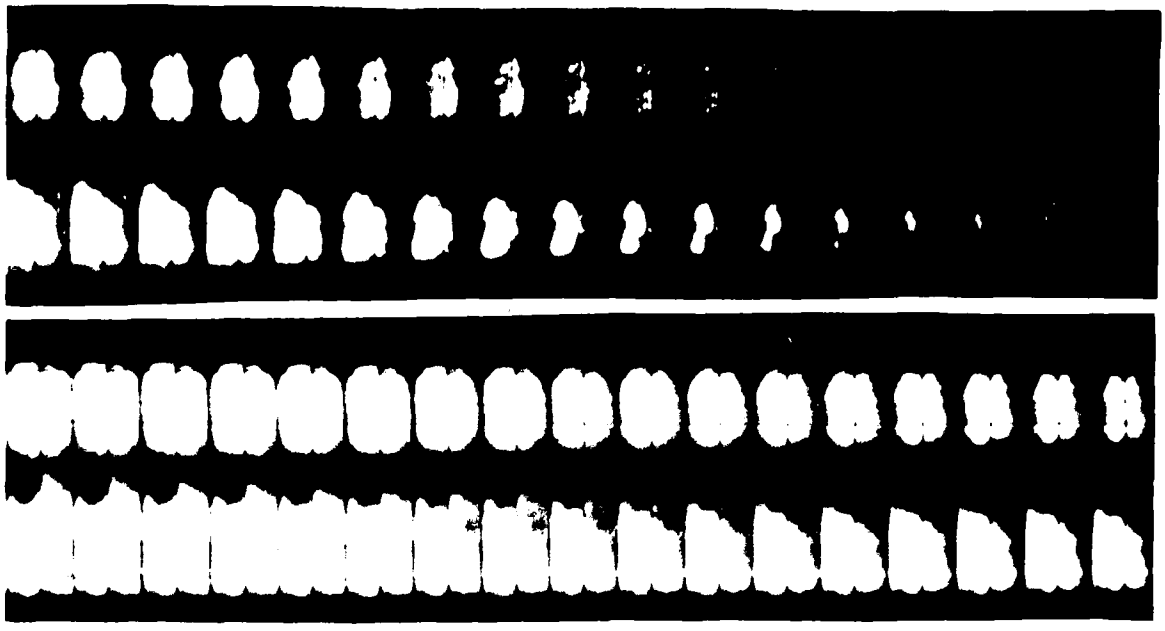

Figure 21. Propagation of the Luminous Flame Front, ALCLO Igniter

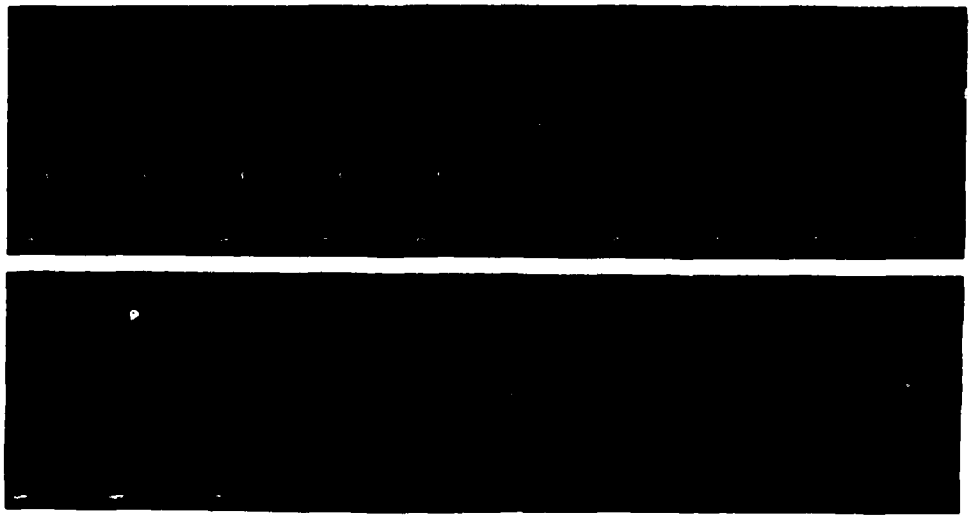

Figure 22. Propagation of the Luminous Flame Front, BP RIP Igniter

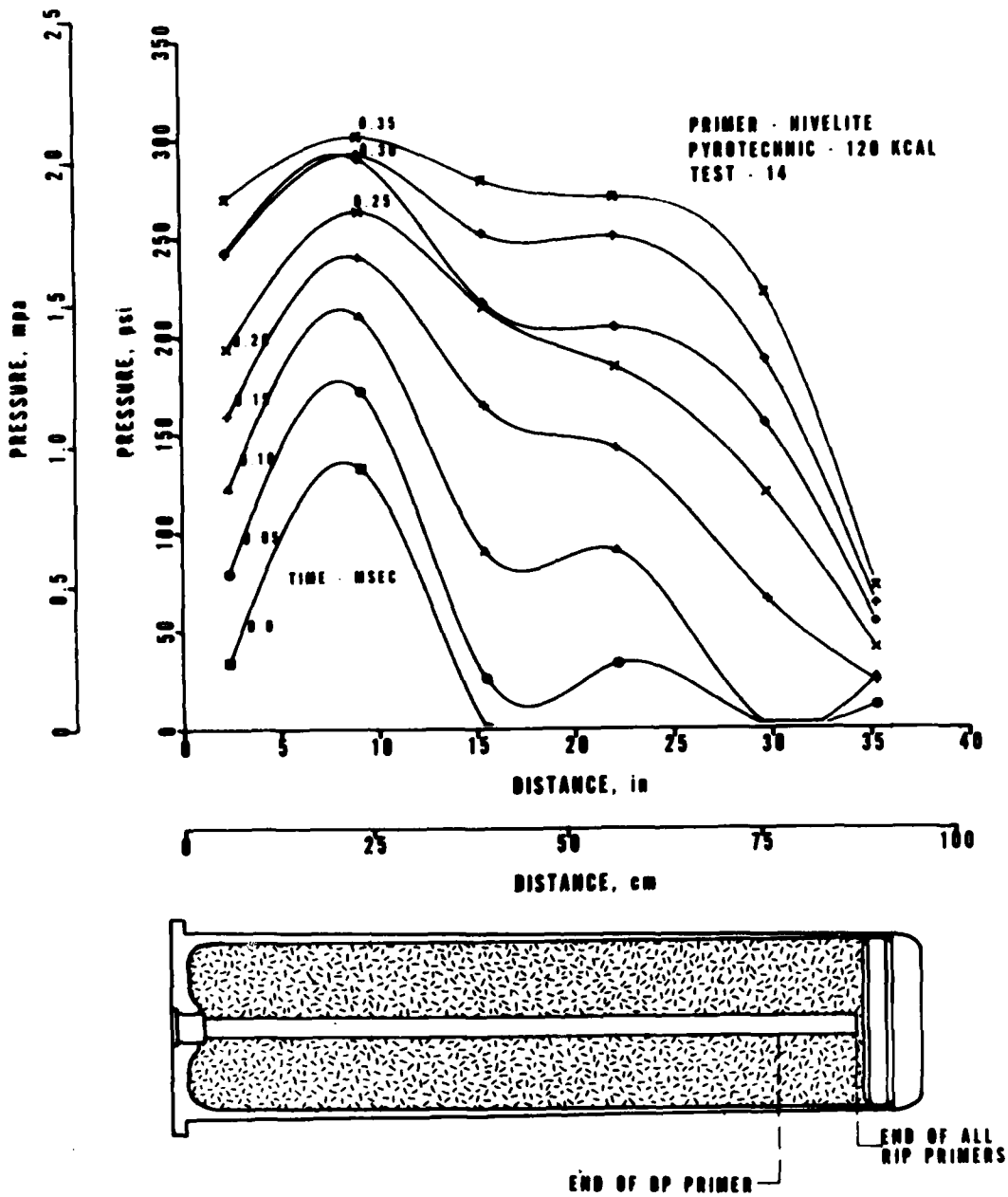

Figure 23. Pressure Distribution in an Inert Bed, HIVELITE (120 kcal) Igniter

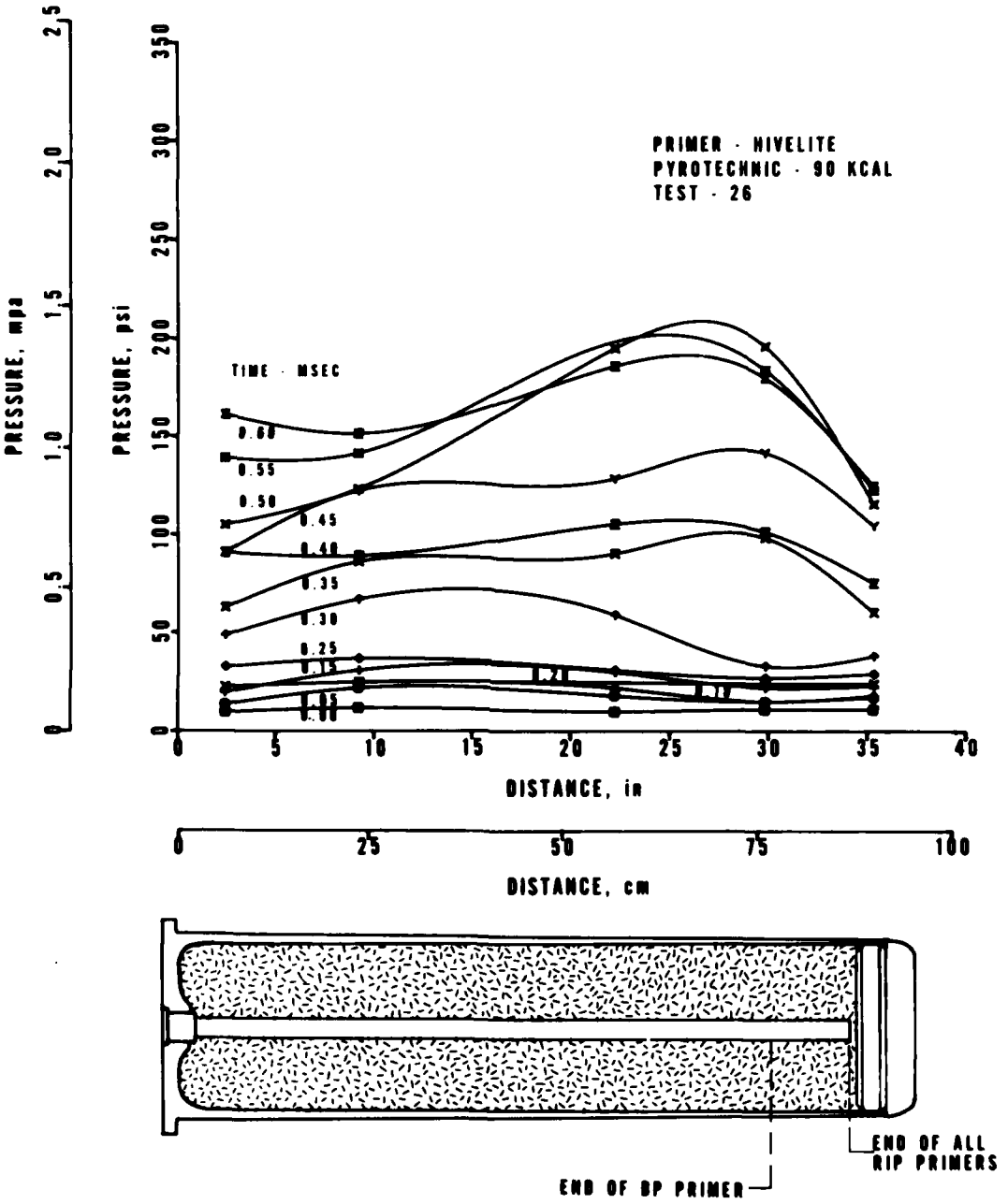

Figure 24. Pressure Distribution in an Inert Bed, HIVELITE (90 kcal) Igniter

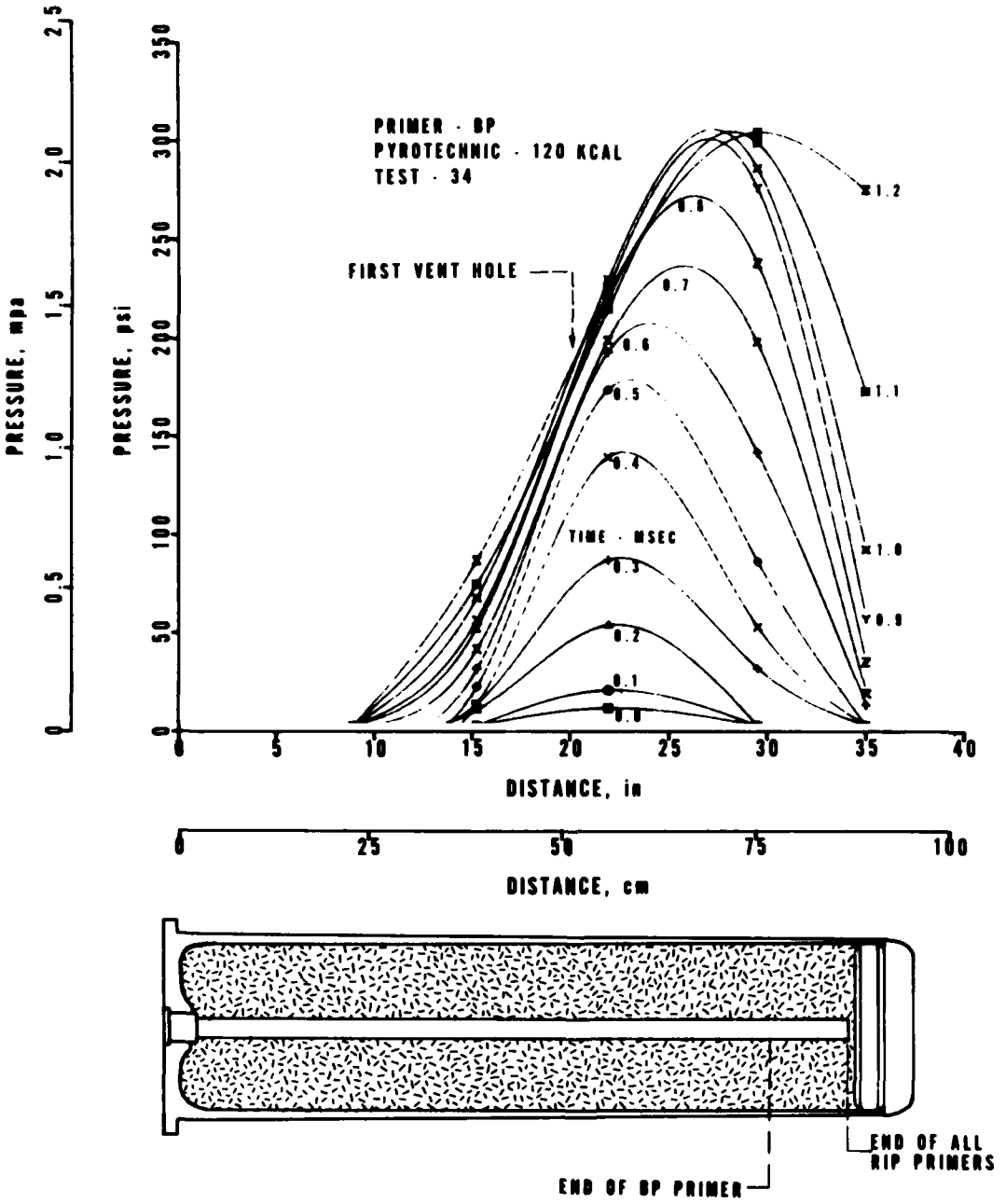

Figure 25. Pressure Distribution in an Inert Bed, BP Igniter

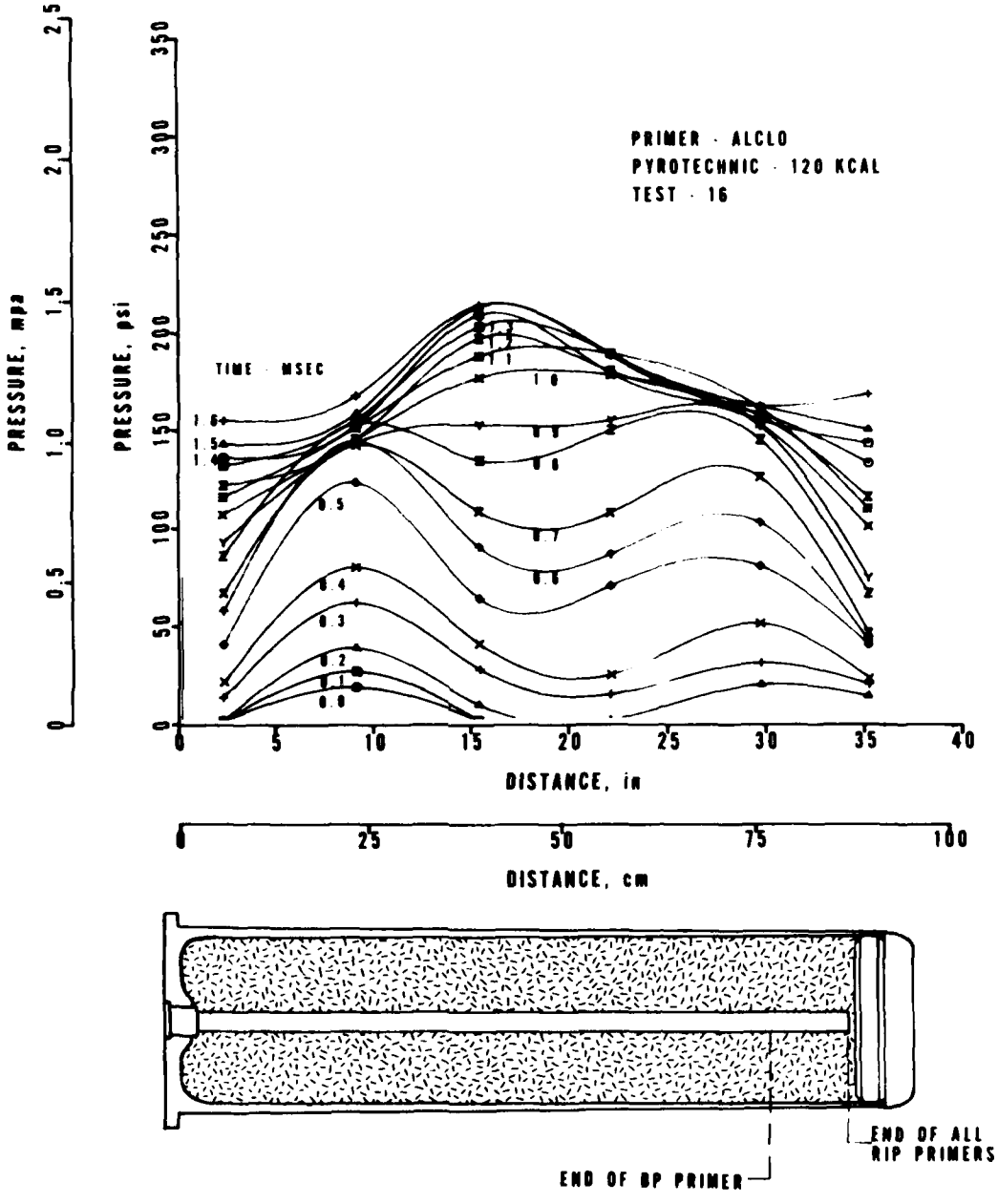

Figure 26. Pressure Distribution in an Inert Bed, ALCLO Igniter

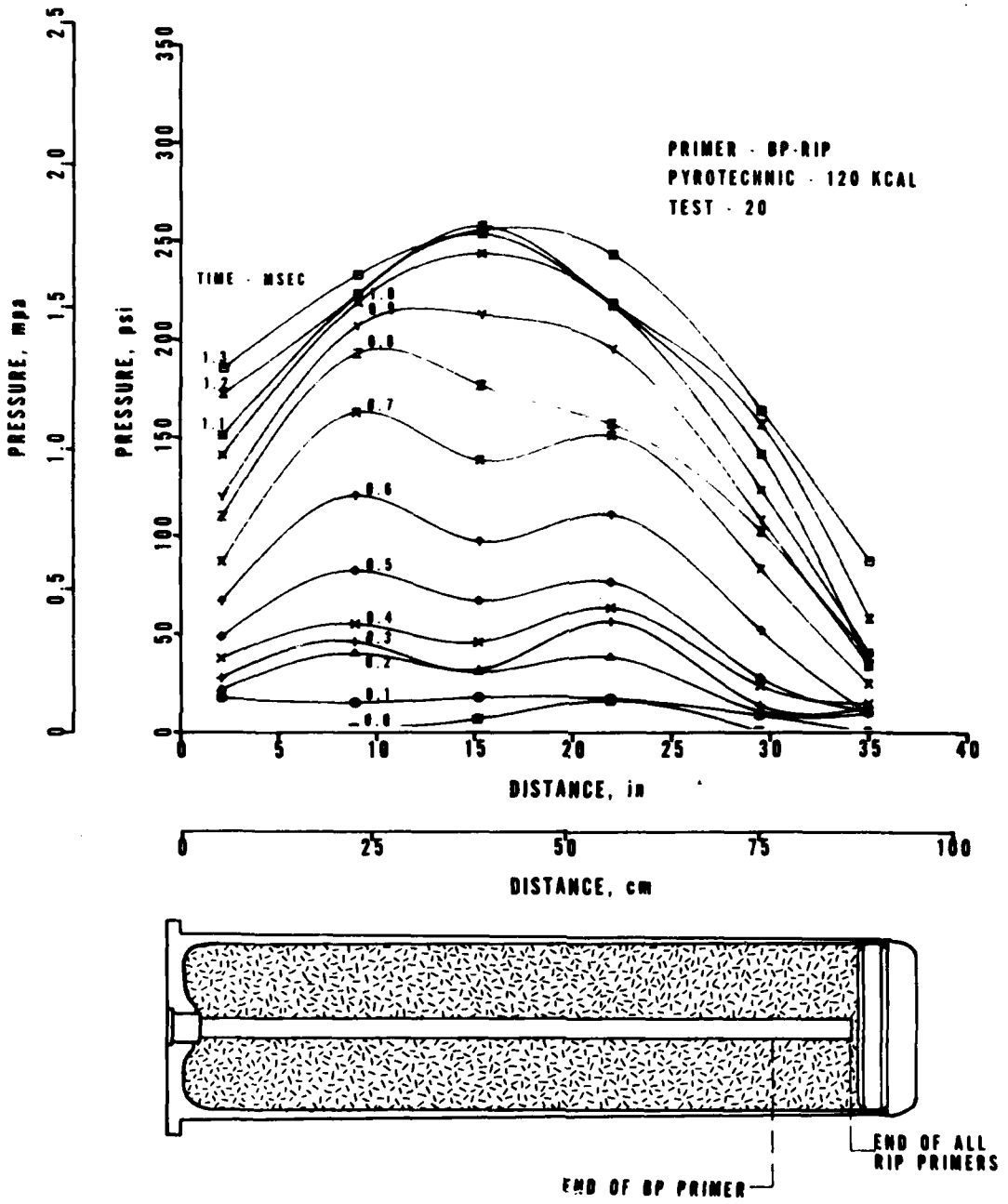

Figure 27. Pressure Distribution in an Inert Bed, BP RIP Igniter

DISTRIBUTION

Assistant Secretary of Defense (R&E)
Washington, DC 20301

Director of Defense Research and
Engineering (OSD)
Washington, DC 20301

Assistant Secretary of the Navy
(Research and Development)
Department of the Navy
Washington, DC 20350

Chief of Naval Research
Department of the Navy
Arlington, VA 22217

Director of Naval Laboratories
Department of the Navy
Washington, DC 20360

Chief of Naval Operations
Department of the Navy
Washington, DC 20360

Chief of Naval Material
Department of the Navy
Washington, DC 20360

Commander
Naval Sea Systems Command
Washington, DC 20360
ATTN: SEA-03
SEA-033
SEA-0331
SEA-034
SEA-035
SEA-04
SEA-04J
SEA-653
SEA-6531
SEA-653C
SEA-65313C
SEA-99

Commander
Naval Air Systems Command
Washington, DC 20360

DISTRIBUTION (Continued)

Commanding Officer
Air Force Armament Test Laboratory
Eglin AFB, FL 32542
ATTN: O. K. Heiney
Technical Library

Armaments Command
Rock Island Arsenal
Rock Island, IL 61200

Commanding General
U.S. Army Material Command
Washington, DC 20315

Commanding Officer
Watervliet Arsenal
Watervliet, NY 12189
ATTN: Technical Library

Commanding Officer
Frankford Arsenal
Bridge-Tacony Streets
Philadelphia, PA 19137

Commanding Officer
Picatinny Arsenal
Dover, NY 07801
ATTN: Dr. J. Picard
H. Hassman
C. Lenchitz
Dr. H. Fair
Dr. D. Downs

Director
Army Ballistics Research Laboratories
Aberdeen Proving Ground, MD 21005
ATTN: Dr. J. R. Ward
J. M. Frankle
Dr. I. W. May
A. W. Horst
T. Baran
Dr. D. Kooker
Dr. K. White
Technical Library

Commanding Officer
Aberdeen Proving Ground
Aberdeen, MD 21005

DISTRIBUTION (Continued)

Director
Advanced Research Projects Agency
Department of Defense
Washington, DC 20301

Director
Naval Research Laboratory
Washington, DC 20390

Commander
Naval Weapons Center
China Lake, CA
ATTN: D. Weathersby

Commander
Naval Ordnance Station
Indian Head, MD 20640
ATTN: S. E. Mitchell
T. C. Smith
C. Gautier
L. Roseborough
C. Irish
R. Montoya
Technical Library

Commanding Officer
Naval Ordnance Station
Louisville, KT 40214

Superintendent
U.S. Naval Academy
Annapolis, MD 21402

Commandant
Headquarters, U.S. Marine Corps
Washington, DC 20380

Commanding General
Marine Corps Development and
Educational Center
Quantico, VA 22134
ATTN: Head, Mid Range Branch
Chief, Ground Operations Division

DISTRIBUTION (Continued)

Superintendent
Naval Postgraduate School
Monterey, CA 93940

Commanding General
Army Material and Mechanics Research Center
Watertown, MA 02172

Commanding Officer
U.S. Army Material Development and
Readiness Command
5001 Eisenhower Ave.
Alexandria, VA. 22304

Commanding Officer
Army Research Office
Arlington, VA 22207

Commanding Officer
Army Research Office (Durham)
Box CM, Duke Station
Durham, NC 27706

University of Illinois
Urbana, IL 61901
ATTN: Dr. H. Krier

Calspan Corporation
Buffalo, NY 14200
ATTN: E. B. Fisher

Defense Documentation Center
Cameron Station
Alexandria, VA 22314 (2)

Local:

DG06 (2)
E23 (Seplow)
E41
G
G02 (Soper)
G21 (Brandts) (Perrine) (Blankenship)
G30 (Payne) (Monn) (Kell)
G302 (Kitterman)
G33 (Boyer) (45)
G61 (Jablovskis)

DISTRIBUTION (Continued)

G62 (Packett)
N41 (Ramsburg) (Hammer)
X210 (2)
X211 (2)